Available online at www.sciencedirect.com
ScienceDirect
Trans. Nonferrous Met. Soc. China 34(2024) 3789−3821
Transactions of Nonferrous Metals Society of China
www.tnmsc.cn

Research and development of advanced copper matrix composites

Zhu XIAO[1,2], Yan-jun DING[1], Ze-jun WANG[1], Yan-lin JIA[1,2], Yan-bin JIANG[1,2], Shen GONG[1,2], Zhou LI[1,2]

1. School of Materials Science and Engineering, Central South University, Changsha 410083, China;
2. Key Laboratory of Non-ferrous Metal Materials Science and Engineering, Ministry of Education, Changsha 410083, China

Received 29 June 2024; accepted 2 December 2024

Abstract: Copper matrix composites (CMCs) offer promising applications by combining the functional characteristics of copper with composite phases. With the rapid advancement in aerospace, microelectronics, and intelligent terminal engineering, the demand for CMCs with superior mechanical and electrical properties has become increasingly critical. This paper reviews the design principles, preparation methods, microstructures and properties of some typical CMCs. The existing form of composite phases in the Cu matrix and their effects on microstructure evolution and comprehensive properties are summarised. Key underlying mechanisms governing these enhancements are discussed. The results provide a systematic understanding of the relationship between reinforcement phases and properties, offering insights for the future development of CMCs aimed to achieve much better comprehensive properties. The paper concludes by outlining the development trends and future outlook for the application of CMCs.

Key words: copper matrix composites; composite principle; reinforcement phase; strength; conductivity

1 Introduction

Copper matrix composites (CMCs) combined with the characteristics of copper matrix and the unique functional characteristics of composite phase, possess excellent comprehensive properties, such as outstanding electrical and thermal conductivities, good corrosion and wear resistances, superior hardness, high temperature softening resistance and magnetic shielding resistance [1,2]. In recent years, CMCs have been widely applied in the fields of high-speed rail transit, charging piles, ultra-high voltage transmission and transformation, advanced microwave radar guidance, medical imaging equipment, direct current relay, 5G mobile communication technology, resistance welding, plasma acting components in nuclear fusion system and combustion chamber bushing [3].

With the rapid development of modern industrial technology and new quality productive force systems, the demand for materials with both high electrical conductivity and mechanical properties are growing exponentially. The high-strength and high-conductivity CMCs fabricated by adding reinforcements into the Cu matrix attract more and more attention. However, the enhancement of the strength of copper by adding reinforcement often comes at the expense of the decrease of conductivity [4,5]. This trade-off is particularly problematic because conductivity is a critical parameter in many applications of CMCs. For instance, in electrical connectors and power transmission systems, maintaining high conductivity and good mechanical properties is essential for efficient and reliable operation. The challenge of simultaneously improving both the strength and electrical conductivity of CMCs has

Corresponding author: Zhou LI, Tel: +86-731-88830264, E-mail: lizhou6931@163.com
DOI: 10.1016/S1003-6326(24)66641-0

become a major focus in current research, driving significant advances in material design and processing techniques [6]. However, despite these advances, there remains a lack of a systematic summary of the composite principles and the underlying mechanisms that govern the performance of high-strength and high-conductivity CMCs.

In this paper, CMCs are classified into three main categories: particle-reinforced CMCs, micro-composite copper alloys, and Cu−carbon composites. Each category represents a different approach for reinforcement, offering unique benefits and challenges in terms of the material properties and processing. The preparation methods of CMCs, including stir casting [7,8], traditional powder metallurgy (TPM) [9−11], hot pressing (HP) [12], friction stir processing (FSP) [13], severe plastic deformation (SPD) [14,15], infiltration [16], compound casting process [17] and spark plasma sintering (SPS) [18] are introduced. According to the classification of reinforcement phases, the composite principle, fabrication process and the enhancement impact of various typical CMCs are reviewed. Furthermore, the existing form of composite phases in the Cu matrix, their influence on microstructure evolution, the comprehensive properties of the CMCs, and the underlying mechanisms are discussed. Finally, the development and prospect of CMCs are presented. This paper is expected to provide a theoretical basis and technological support for the design and fabrication of CMCs with much better comprehensive properties.

2 Particle-reinforced copper composites

At present, the particle-reinforced CMCs are studied commonly and the fabrication process is relatively mature in application. Compared with copper-based alloys, particle-reinforced CMCs have attracted much attention due to their higher specific strength and better high-temperature strength [19−23]. The enhancement of mechanical properties of particle-reinforced CMCs are closely related to the particle size, volume fraction and distribution state of reinforced particles, which can be controlled by adjusting the preparation conditions to avoid the aggregation of the particles in the copper matrix. The dispersed particles in the copper matrix can effectively prevent the slipping of dislocation and have a slight effect on electron scattering [24]. Thus, the particle-reinforced CMCs exhibit outstanding mechanical performance and electric conductivity, and the mechanical properties can be maintained even at elevated temperatures.

The most common preparation method for particle-reinforced CMCs is powder metallurgy, which contains the following processes: mixing, moulding, sintering and processing. Although the process of powder metallurgy is complicated, it has the advantages of easy mass production and relatively stable material properties of particle-reinforced CMCs. In recent years, the in situ reactive synthesis of materials has become one of the novel methods to prepare particle-reinforced CMCs and other ceramic-metal composites due to the advantages of simple processes, good material properties, low product cost and near-final moulding. The key technical principle of in situ reactive synthesis is to select appropriate reaction agents and suitable fabrication parameters according to the material design requirements. Thus, the fine reinforcing particles are generated by the redox reaction of metals and alloys in a tailored approach. The ceramic particles can be distributed evenly and the interface between ceramic particles and the alloy matrix is clean without contaminations and reaction products [25]. So, there is an ideal match between the ceramic particles and the alloy matrix. The interface bonding and thermodynamic stability of the in situ reactive synthesis particle-reinforced CMCs can meet the requirement for use in certain situation. As the Al_2O_3, SiC, and TiB_2 particles reinforced CMCs have been studied extensively and have the most promising application prospects, the research status of preparation technology and performance characteristics of these CMCs are summarized in this paper.

2.1 Cu−Al_2O_3 composites

Compared with copper, Cu−Al_2O_3 composites possess higher strength and hardness, superior high-temperature softening resistance and high-temperature stability, and their softening temperature is as high as 900−1000 °C, while their electrical conductivity only decreases slightly [26]. As typical dispersion-strengthened CMCs with high strength and high electrical conductivity, Cu−Al_2O_3

composites have a broad application prospect in resistance welding electrodes, silver replacement contact, lead wire, microwave tube structure material IC lead wireframe and mould of continuous caster [24]. The common preparation of Cu−Al_2O_3 composites includes the internal oxidation method and mechanical alloying method. The properties of Cu−Al_2O_3 composites fabricated by the two methods in different states are listed in Table 1 [27−31]. Related investigations of the properties of Al_2O_3-reinforced CMCs confirmed that the wear resistance, hardness and thermal stability performance of CMCs were enhanced with the increase of the Al_2O_3 content in the copper matrix [32].

Figure 1 shows TEM images of the Cu−5vol.%Al_2O_3 composite prepared using a combination of high-energy mechanical milling and compact powder extrusion [33]. The extruded rod features equiaxed grains, with over half of the grains with the size of 300−560 nm. Figure 1(c) shows a TEM dark field image using part of the

Table 1 Properties of dispersion strengthened CMCs

Fabrication method	Composition	σ_b/MPa	$\sigma_{0.2}$/MPa	Elongation/%	Electrical conductivity/%(IACS)	Ref.
Internal oxidation	Cu−0.6wt./%Al_2O_3	290.2	145.9	31.7	75	[29]
	Cu−1.12wt./%Al_2O_3	441	455	22	88	[29]
	Cu−1vol./%Al_2O_3	317	275	15	52	[27]
	Cu−2.7vol./%Al_2O_3	533	570	25	85	[28]
Mechanical alloying	Cu−0.66wt./%Al_2O_3	522	470	3.9	79.1	[30]
	Cu−4.5vol./%Al_2O_3	522	461	8.2	90	[31]

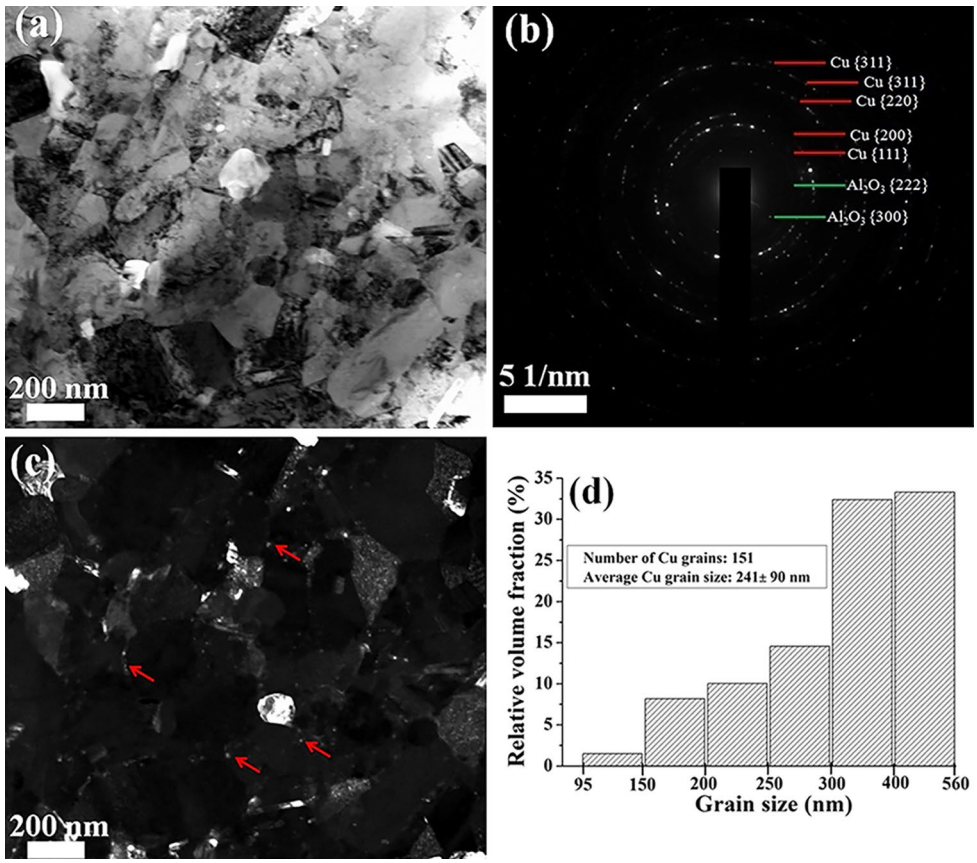

Fig. 1 (a) TEM bright field (BF) image; (b) Selected area electron diffraction (SAED) pattern corresponding to (a); (c) TEM dark field (DF) image corresponding to (a); (d) Cu grain size distribution of extruded UFG Cu−5vol.%Al_2O_3 composite [33]

Al_2O_3 diffraction ring from Fig. 1(b), revealing that Al_2O_3 nanoparticles (5−20 nm) are mainly distributed along the grain boundaries. This inhomogeneous distribution provides three beneficial effects: (1) stabilization of the ultrafine structure at elevated temperatures; (2) minimization of electron scattering at Cu/Al_2O_3 interfaces; (3) improvement in strength. These positive effects suggest that nanocrystalline ultrafine-grained Cu, with second-phase nanoparticles locating around its grain boundaries, can exhibit superior thermal stability, strength, and electrical conductivity. The composite demonstrates a high tensile yield strength of 486 MPa and an electrical conductivity of 80% IACS. However, a critical drawback of fabricating Al_2O_3-reinforced CMCs via powder metallurgy is the susceptibility of copper powder to oxidation and its poor wear resistance. Studies have shown that silver coating on the surface of Cu−Al_2O_3 powder can effectively enhance the oxidation resistance of copper powder and improve the wettability of Al_2O_3, due to the enhancement effect of the dispersion of nanoparticles [34,35]. Additionally, by combining the internal oxidation method with mechanical alloying, Cu−3.6vol.% Al_2O_3 dispersion-strengthened alloy was prepared by mechanically alloying internally oxidized Cu−Al powder [36]. The results show that this combined method can completely oxidize the residual aluminum during internal oxidation within 10−20 h, whereas mechanical alloying alone requires more than 40 h. After milling, the size of the Al_2O_3 particles decreased from 46 to 22 nm. Due to the refinement of Al_2O_3 particles and the in-situ oxidation of residual aluminum, the average hardness and electrical conductivity of the mechanically alloyed powder after milling in argon reached HV 172.2 and 82.1%(IACS), respectively, while the unmilled alloy showed an average hardness and conductivity of HV 119.8 and 74.1% (IACS), respectively.

The typical process for preparing Cu−Al_2O_3 composites via internal oxidation can be summarized as follows: Cu−Al melting →water/gas atomizing powder →preparation of the oxidant → mixing alloy powders with the oxidant → high-temperature oxidation (800−1000 °C) in a sealed container → crushing → isostatic pressing of billets → ingot packaging → vacuum sealing → hot extrusion → cold drawing → final products. Cu−Al_2O_3 composites prepared by the internal oxidation method exhibit superior comprehensive properties compared to those prepared by the mechanical alloying method.

The Cu−2.7vol.%Al_2O_3 composites were produced via internal oxidation, revealing two mechanisms that enhance the material's yield strength: the Hall−Petch mechanism at room temperature and the strong pinning effect of alumina particles on grain and sub-grain boundaries at high temperatures [37]. As shown in Fig. 2, numerous Al_2O_3 particles are distributed in the Cu matrix, mostly with spherical shape and diameters ranging from 10 to 50 nm, along with a few triangular and irregular particles (Fig. 2(a)). Additionally, due to the preferential diffusion of oxygen atoms and weaker binding forces during internal oxidation, coarse rod-like Al_2O_3 particles with the size of about 200 nm are found at the grain boundaries. Both spherical and rod-like Al_2O_3 particles are γ-Al_2O_3. After annealing at 900 °C, the subcrystalline size is 0.2−0.5 μm, and the average grain size is about 0.4 μm (Figs. 2(e, f)) [37]. Additionally, Cu−Al_2O_3 composites prepared by the internal oxidation method exhibit the most stable microstructure and performance during high-temperature annealing. The significant difference in elastic modulus between Cu−Al_2O_3 and copper inhibits the grain growth of Cu−Al_2O_3, which is the primary reason for the increased softening temperature of Cu−Al_2O_3 composite [26].

2.2 Cu−TiB_2 composites

The research on TiB_2-reinforced CMCs has become a hot spot in composites due to the fact that TiB_2 has a high melting point (3225 °C), hardness (34 GPa), elasticity modulus and electrical conductivity. The preparation processes of Cu−TiB_2 composites include the mechanical alloying method, spray deposition method and exothermic dispersion [38−40]. The properties of Cu−TiB_2 composites prepared by different processes are listed in Table 2 [41−45].

In recent years, many works have been carried out to produce in-situ TiB_2 particle reinforced CMCs due to the advantages of clean and compatible interface bond, low cost and simplified process [40,41]. The Cu−TiB_2 composites prepared by mixed reaction of double melt have excellent comprehensive performance. The Cu−B and Cu−Ti

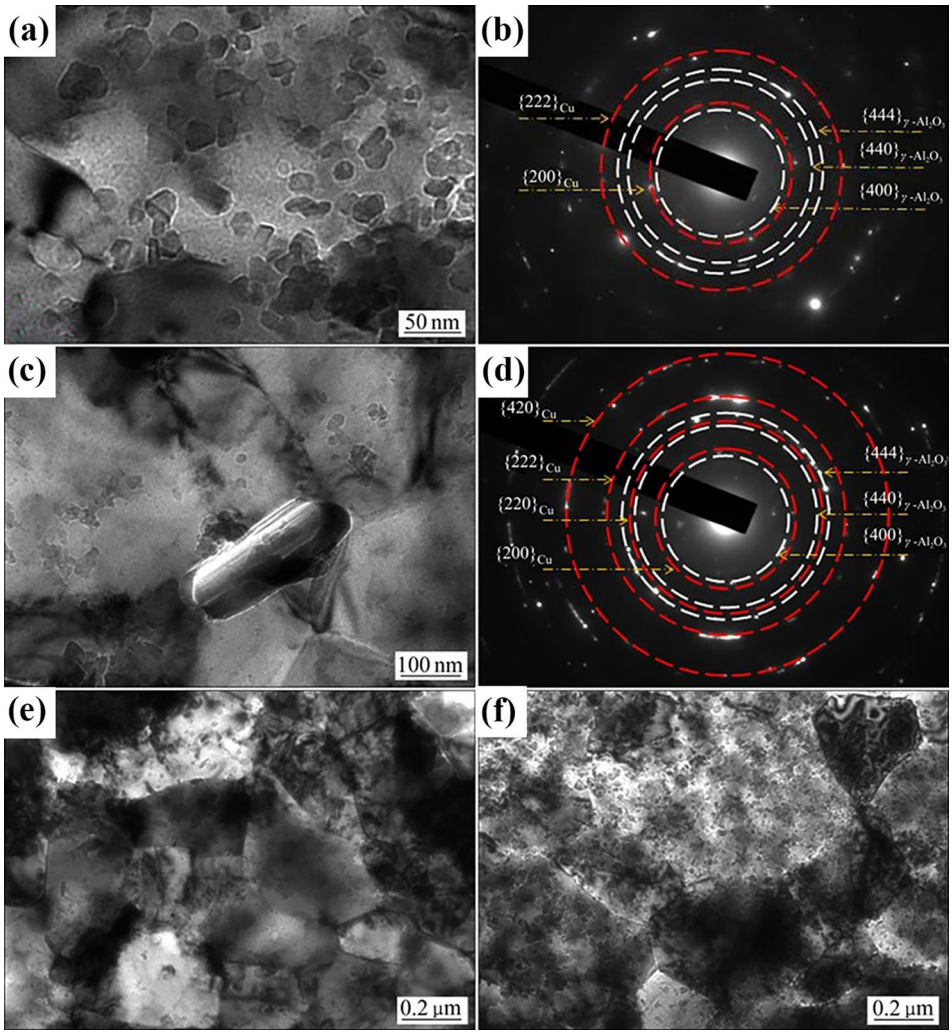

Fig. 2 TEM results of annealed Cu−2.7vol.%Al_2O_3 dispersion Cu: (a) Distribution of Al_2O_3 particles in Cu matrix; (b) SAED pattern of (a); (c) Thick Al_2O_3 particles at grain boundary; (d) SAED pattern of (c); (e, f) BF images of copper alloy annealed 900 °C [37]

Table 2 Properties of Cu−TiB_2 composites prepared by various processes

Fabrication method	Composition/ wt.%	Processing method	σ_b/ MPa	$\sigma_{0.2}$/ MPa	Elongation/ %	Electrical conductivity/%(IACS)	Ref.
In-situ casting process	Cu−0.5TiB_2	Cold-rolling	414.4	391.4	1.17	89.64	[41]
	Cu−1TiB_2	Cold-rolling	423.5	397.5	1.09	8583	[41]
	Cu−1.5TiB_2	Cold-rolling	442.5	409.8	0.86	73.43	[41]
Reactive spray deposition	Cu−2TiB_2	Cold-rolling	401	−	10.2	83.5	[42]
Reactive hot pressing	Cu−3TiB_2	−	438±23	−	23.2±1.8	−	[43]
Vacuum arc melting	Cu−2.6TiB_2	Aging at 475 °C for 4 h	246	−	38.3	87	[44]
Powder metallurgy	Cu−2.6TiB_2	Aging at 475 °C for 4 h	226	−	24.6	84.6	[44]
Mechanical alloying	Cu−0.5TiB_2	−	248	130	50	88.4	[45]
	Cu−1TiB_2	−	252.5	140	44	86	[45]
	Cu−3TiB_2	−	278	160	28	84.2	[45]
	Cu−5TiB_2	−	283	180	25	83.3	[45]

alloys are melted in crucibles respectively by an intermediate frequency melting furnace at an inert gas atmosphere. The in-situ reaction of $Ti+2B\rightarrow TiB_2$ takes place at a turbulent mixing melt flow through the melt transport channel. Finally, Cu−TiB_2 composite melt is pumped out through the nozzle and cast in a cooled copper mould. The Cu−Ti and Cu−B melts thoroughly and uniformly mixed in a turbulent state are the key point of the process. The composite is then strengthened while the generation of nanoscale TiB_2 particles distributed evenly in the matrix is sufficient.

Figure 3 shows the SEM images of Cu−TiB_2 composites prepared by a mixed reaction of double melt. As demonstrated that the agglomeration and growth process of TiB_2 particles and numerous fine TiB_2 particles less than 50 nm are found in the matrix, indicating that Cu−TiB_2 composites with a uniform structure and fine TiB_2 particles can be fabricated under reasonable control of reaction conditions. The thermodynamic study of the mixed reaction of double melt of Cu−Ti and Cu−B shows that TiB_2 is the main strengthening phase as TiB_2 has a lower Gibbs free energy than TiB phases. The TiB_2 particles mainly nucleate near the interface. The more interfaces the double melt reacts, the higher the nucleation of TiB_2 particles will be, and the easier it is to form nanoscale TiB_2 particles [47]. The main strengthening mechanisms of Cu−TiB_2 composites include refinement strengthening, dispersion strengthening, load transfer strengthening and dislocation strengthening caused by geometric constraints during deformation and thermal mismatch dislocation strengthening [48]. The contribution of dispersion strengthening to the strength increases with the increase of TiB_2 content. The main factors affecting the conductivity of Cu−TiB_2 composites are the residual solute elements Ti and B due to the side reactions and content and size of TiB_2 particles [48].

Figure 4 presents the TEM characterization results of in situ Cu−TiB_2 composites fabricated using solid−liquid (S−L) and liquid−liquid (L−L) reactive spray deposition methods [42]. In contrast, SAED analysis of the L−L sample identified particles as TiB_2, with few B particles was detected. The rapid cooling rate in the S−L reaction resulted in a high solid volume fraction in the droplet, leading to difficulties in adherence to the billet's top layer and causing the formation of micropores. Table 3 compares the electrical conductivity, hardness, tensile strength, and elongation of the S−L and L−L samples. The mechanical properties of the L−L samples are superior to those of the S−L samples.

The powder metallurgy method effectively addresses the issue of poor wettability between ceramic particles and the melt matrix, thereby uniformly dispersing micron- and nano-sized particles within the matrix [40,45]. This method also allows for the production of Cu−TiB_2 composites with a high TiB_2 content. Additionally, mechanical alloying combined with subsequent cold pressing and heat treatment processes enables the in-situ formation of TiB_2 from copper, titanium, and boron metal powders, successfully producing TiB_2-reinforced CMCs [40]. After 26 h of ball milling, only the Cu_4Ti phase forms through the reaction of copper and titanium, which is subsequently replaced by TiB_2 during the cold pressing and heat treatment processes. This indicates that mechanical alloying enhances the in-situ development of TiB_2 in the structure, which can be explained by the reaction of $Cu_4Ti+2B=TiB_2+4Cu$ [40].

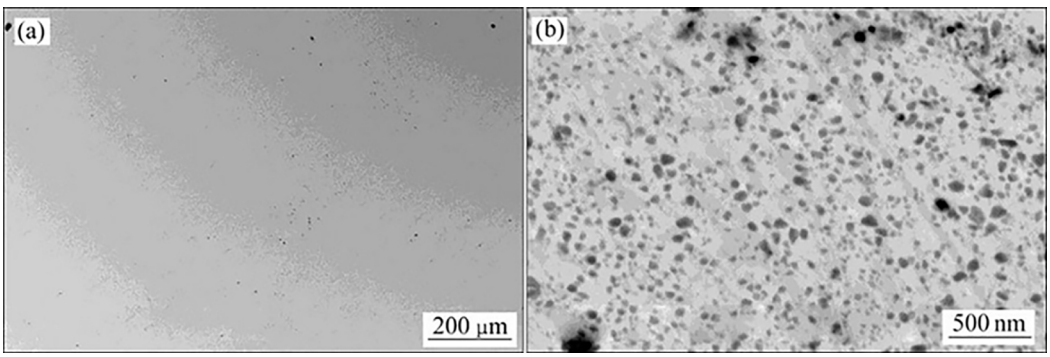

Fig. 3 SEM images of Cu−TiB_2 composites prepared by mixed reaction of double melt: (a) Low-magnification; (b) High-magnification [46]

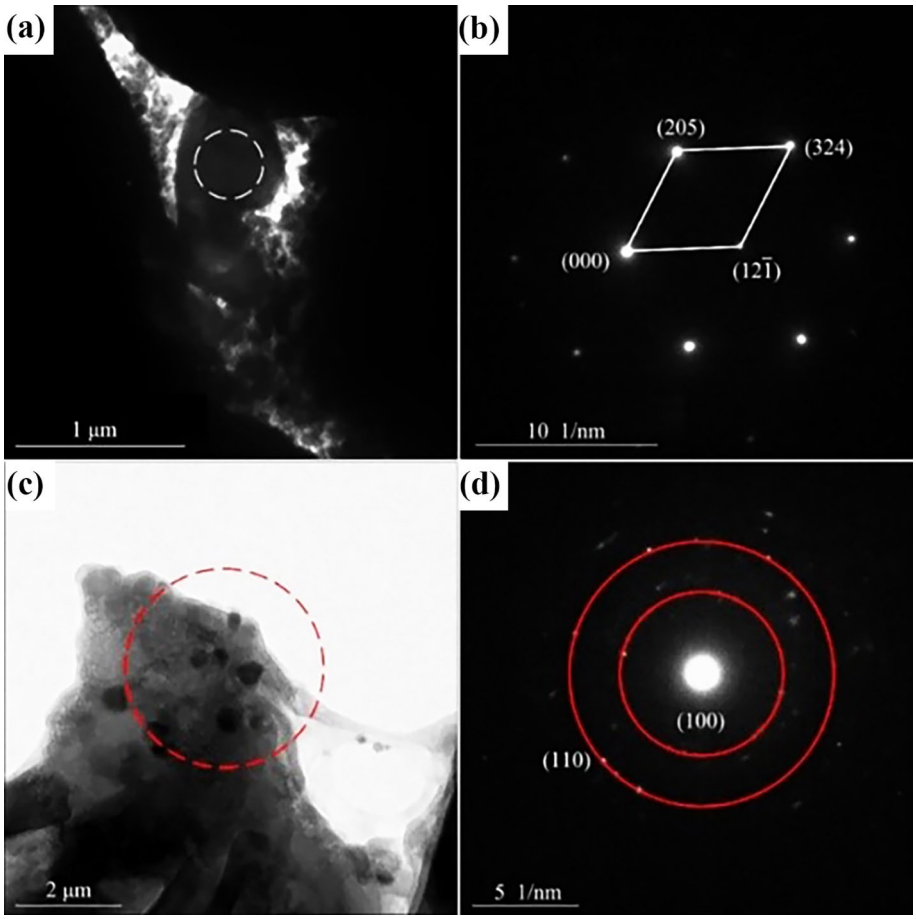

Fig. 4 TEM images of S−L and L−L samples: (a, b) BF image of B powder in S−L sample and corresponding SAED pattern; (c, d) BF image of TiB_2 particles in L−L sample and corresponding SAED pattern [42]

Table 3 Electrical conductivity, hardness, tensile strength and elongation of S−L and L−L samples [42]

Sample	Electrical conductivity/%(IACS)	Hardness (HB)	Tensile strength/MPa	Elongation/%
As-deposited S−L sample	12.5	87±1.6	242	10.2
As-deposited L−L sample	82.5	68±2.2	287	24.2
Deformed S−L sample	20.2	140±1.8	520	4.4
Deformed L−L sample	83.5	100±1.3	401	10.2

2.3 Cu−SiC composites

Cu−SiC composites, as a type of ceramic phase reinforced structure-function integrated CMCs, have been widely applied in the fields of electronic packaging, electrical contact, aerospace, and friction industry because of their excellent electrical and thermal conductivities, superior mechanical properties, low thermal expansion coefficient as well as good wear and corrosion resistances [4,49−51]. However, it is challenging to combine the SiC and copper matrix by conventional methods due to their poor wettability. The powder metallurgy (PM) and interface modification methods are commonly used to prepare SiC-reinforced CMCs, and these methods are often employed simultaneously [52]. The relevant parameters and properties of the SiC-reinforced CMCs studied by some researchers are listed in Table 4 [49,53,54].

The size and distribution of the reinforcing phase within the matrix affect the microstructure and properties of dispersion-strengthened copper alloys significantly. Cu−SiC nanocomposites, prepared by conventional sintering processes, can enhance the mechanical properties through extending milling time and promoting densification. Prolonging milling time notably refines the grain

size of the composites and ensures a more uniform distribution of nanoparticles [25]. As shown in Fig. 5, near-spherical SiC_p particles, ranging from 50 to 200 nm, are dispersed within the grains and distributed along the grain boundaries of the Cu/SiC_p composites. Figure 5(d) presents a TEM image of the interface between SiC_p particles and the Cu matrix, illustrating that Cu matrix tightly bonds with the SiC_p particles, indicating strong interface bonding. This demonstrates that mechanical alloying and in-situ formation effectively enhance the bonding between SiC_p particles and the copper matrix. As the SiC_p content increases, the size of SiC_p particles also grows, with larger particles appearing at grain boundaries. This is due to the high Si content, leading to partial segregation of Si within the Cu−Si powder, and resulting in more Si atoms at the grain boundaries. During high-temperature heat treatment, SiC_p particles initially form at these boundaries through solid−solid diffusion reactions, effectively reducing the probability of dynamic recrystallization during thermal deformation. Figure 6 presents the STEM and HADDF images of the Cu−1vol.%SiC_p composite. The images indicate that during the high-temperature in-situ carbonization process, a small amount of Si is dissolved in the copper matrix, and few SiC_p phase is observed during the high-temperature solid−solid diffusion reaction. These residual Si particles are subsequently oxidized into nano-sized SiO_2 particles during the internal oxidation process, thereby improving the electrical

Table 4 Preparation process and related properties of silicon carbide dispersion strengthened CMCs

Fabrication method	Composition	σ_b/MPa	$\sigma_{0.2}$/MPa	Elongation/%	Ref.
Powder metallurgy	Cu−4vol.%SiC	410	318	3.4	[49]
HPT process	Cu−10vol.%SiC	730	475	9.1	[53]
	Cu−20vol.%SiC	846	661	7.9	[53]
SPS+HPT process	Cu−10vol.%SiC	440	395	2.9	[54]
	Cu−20vol.%SiC	420	385	1.9	[54]

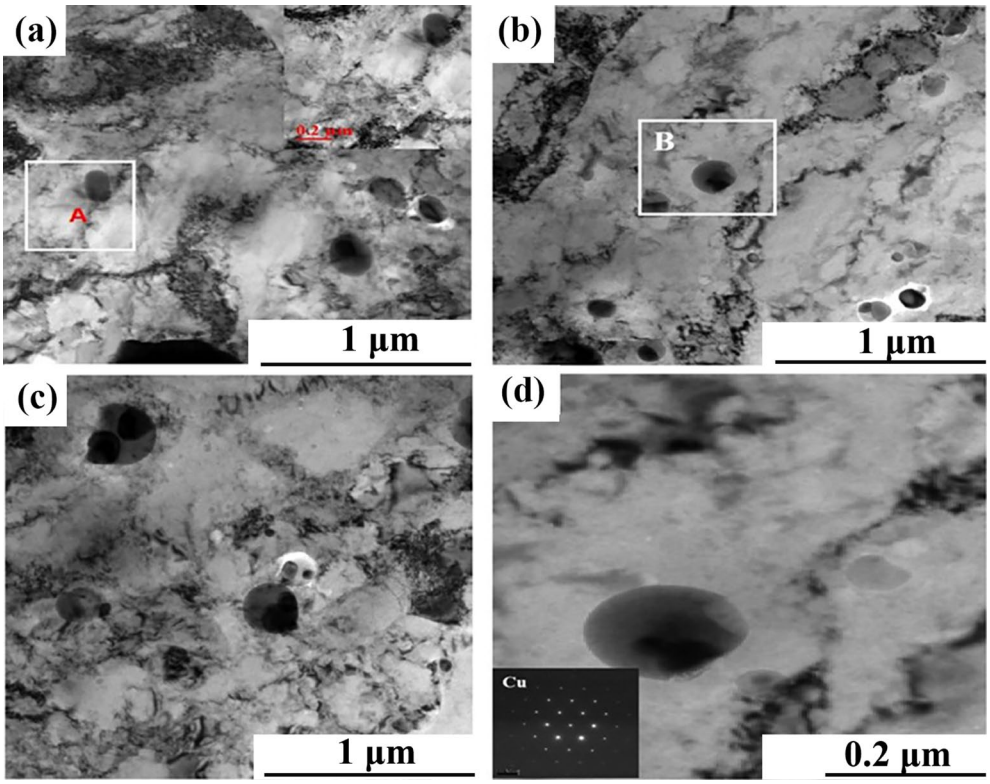

Fig. 5 TEM images of extruded Cu−1vol.%SiC_p composite: (a, c) Central area of composite; (b) Exterior of composite; (d) Enlargement and electron diffraction of B in (b) [25]

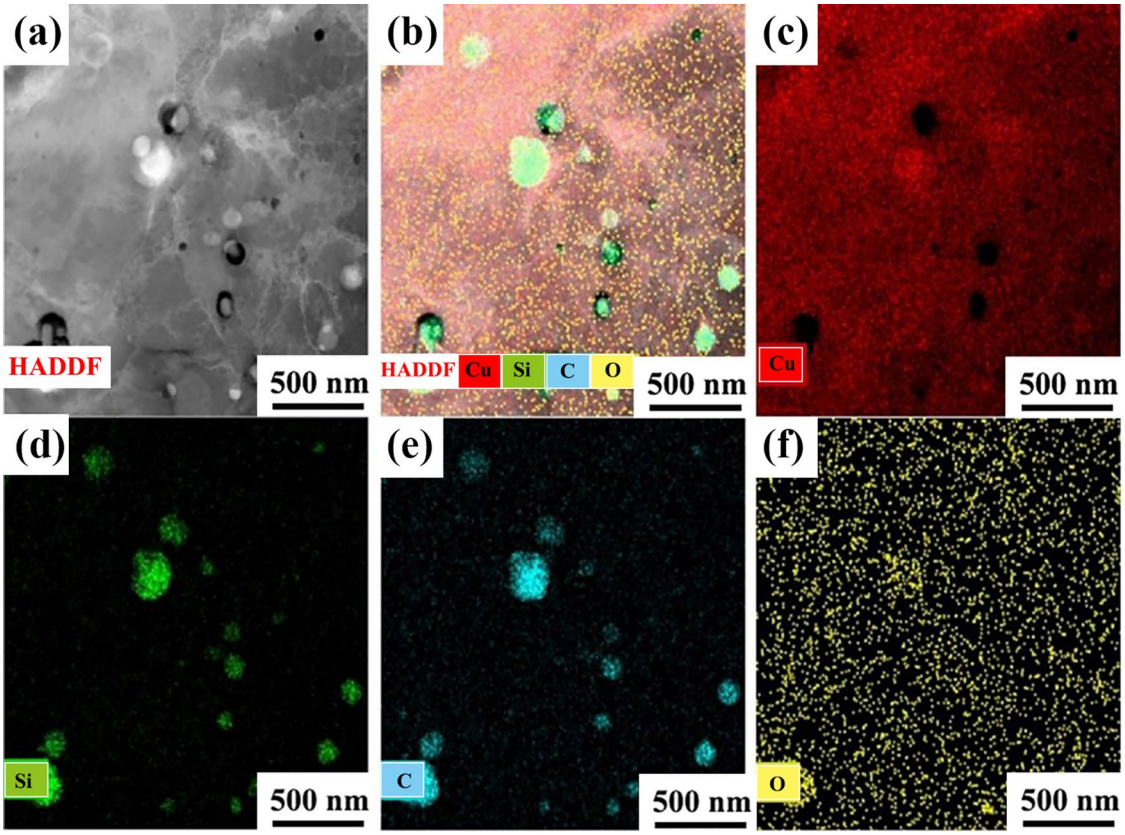

Fig. 6 (a) STEM image of Cu−1vol.%SiC_p composite; (b) HADDF image of Cu−1vol.%SiC_p composite; (c) Analysis of Cu element; (d) Analysis of Si element; (e) Analysis of C element; (f) Analysis of O element [25]

conductivity of the composite. Additionally, hot extrusion deformation can enhance the uniform dispersion of SiC_p particles in composite materials and significantly improve the mechanical and electrical properties of the composites. During the hot extrusion process, initially agglomerated SiC_p particles disperse uniformly within the matrix due to metal flow, without agglomeration occurring. The dispersed SiC_p particles in Cu/SiC_p composite materials play a crucial role in pinning dislocations and substructures. Despite annealing treatments, dislocation cells persist due to the pinning effect of SiC_p particles.

It is widely acknowledged that the interface between SiC and the matrix critically influences the performance of composite [55]. Research indicates that Cu and SiC particles exhibit poor mutual wetting [56]. According to the Cu−SiC phase diagram, silicon dissolves into copper at 5 vol.% solubility at 850 °C, resulting in the formation of graphite layers from excess carbon [57]. The inadequate wetting characteristics within the Cu/SiC system contribute to weak adhesion at residual carbon layers, consequently compromising interface strength. Current strategies to enhance interface strength primarily involve optimizing processing techniques, incorporating active elements, and applying metallic coatings to promote adhesion [4]. Current studies on optimizing the interface of Cu−SiC composites emphasize enhancing interface properties by incorporating trace amounts of active elements. Research findings of first-principles calculations using density functional theory (DFT) indicate that adding Ti alloying elements can significantly strengthen the interface [58]. In other research, to improve interface bonding performance, the electroless copper plating method was used to coat SiC_p, and the SiC_p/Cu composite was then fabricated using the hot-pressed sintering technology [59]. SiC particles were treated at 1200 °C for 60 min in static air. When the plating time exceeded 15 min, Cu nuclei gradually accumulated, resulting in a uniform Cu coating on the SiC_p surface. SiC particles are uniformly dispersed in the Cu matrix when the SiC volume content is below 50%. However, at 60% SiC content, the particles start to aggregate.

2.4 HEA reinforced CMCs

In recent years, the application of high entropy alloys (HEAs) as a reinforcement phase in the preparation of CMCs has attracted the attention of researchers. HEAs are composed of five or more principal elements with concentrations ranging from 5 to 35 at.% [60,61]. High entropy of random mixing of the principle elements can prevent ordered solid solutions and intermetallic phases. Thus, HEAs have mainly consisted of simple solid solutions [62]. Because of a multi-component solid solution, HEAs possess high strength, good structural stability, and exceptional high-temperature strength. In addition, for traditional ceramic particles reinforced CMCs, the low ductility of ceramic particle-reinforced Cu composite is mainly related to the poor interface bonding strength between the Cu matrix and ceramic particles because they cannot completely wet with each other. The microcracks can readily nucleate and propagate in the interfacial region under external load. Moreover, the hard ceramic particles cannot conform to the ductile metal matrix, leading to stress concentration and premature fracture [63]. By comparison, the metallic characteristic of HEAs is beneficial to improving the interfacial strength of MMCs. Therefore, developing new reinforcements with good mechanical compatibility to the Cu matrix becomes a key issue in Cu matrix composite fields. At present, the production of HEA-reinforced CMCs primarily involves techniques such as powder metallurgy, stir casting, additive manufacturing, laser powder bed fusion, spark plasma sintering, and submerged friction stir processing.

Powder metallurgy is the most common method to produce HEA-reinforced CMCs [64]. The mechanical properties and microstructure analysis of AlCoNiCrFe HEA-reinforced CMCs produced by powder metallurgy reveal superior strengthening effects compared to metallic glasses, with no grain growth or formation of intermetallic phases form during the fabrication process, ensuring the stability of the composite structure [65]. Al0.3CoCrFeNi HEA particles can be also used as reinforcement in CMCs, with the advantages focusing on the influence of the transition layer structure on element diffusion behaviour and wear properties, and a notable 30% enhancement in wear resistance can be achieved due to the improved interface bonding strength compared to CMCs lacking a transition layer [66]. Figure 7 presents mapping images of the interfaces of HEA/Cu and HEA/M/Cu composite. In HEA/Cu composites, the presence of Al and O elements at the interface indicates Al diffusion and oxide formation (likely Al_2O_3) during sintering. Conversely, HEA/M/Cu composites exhibit Cr enrichment at the interface, suggesting the formation of $(Al, Cr)_2O_3$ compounds due to sintering conditions. The altered diffusion behaviour within the transition layer structure contributes significantly to the enhancement of hardness and wear resistance of HEA-reinforced CMCs. This approach underscores the potential of the advanced HEA-reinforced metallic matrix composites in high-performance applications.

Compared to powder metallurgy, friction stir processing (FSP) offers significant advantages as a promising method for fabricating the HEA particle-reinforced copper matrix composites, including higher efficiency, environmental friendliness, and cost savings [67,68]. Studies indicate that using FSP

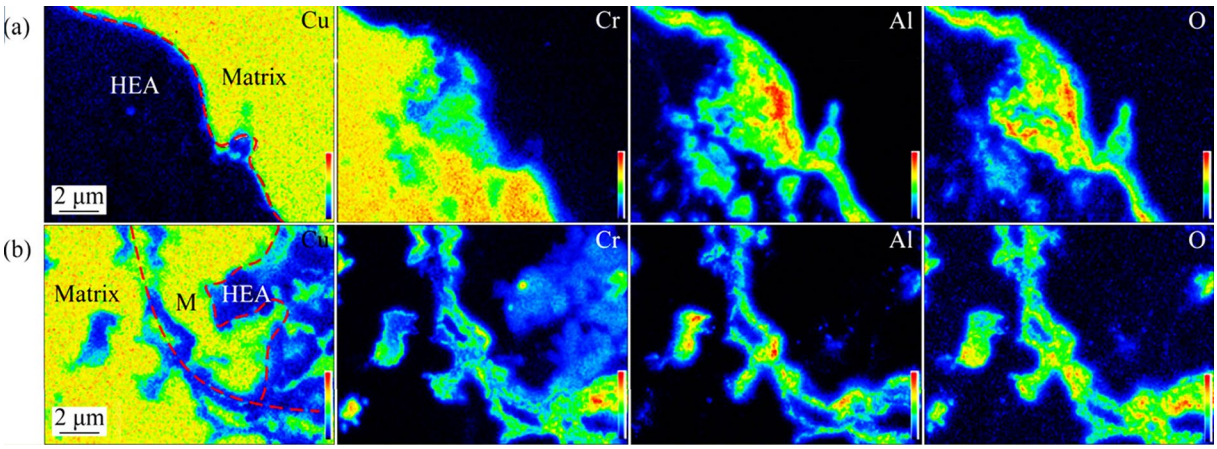

Fig. 7 Elemental mapping images of HEA/Cu (a) and HEA/M/Cu (b) composites at interface by EPMA [66]

to fabricate Cu-based surface composites reinforced by FeCoNiCrAl high-entropy alloy particles results in significant grain refinement of the Cu matrix, with a diffusion layer of about 0.8 μm in thickness at the HEA−Cu interface [67]. These composites exhibit a 69.8% increase in micro-hardness and a 29.7% reduction in wear rate compared to pure Cu, significantly enhancing the wear resistance of the matrix. Furthermore, the composites maintain ductility similar to that of pure Cu, and achieve 87% of the thermal conductivity of pure Cu. This innovation suggests new potential for developing multifunctional structural materials with superior wear resistance, high ductility, and excellent thermal conductivity [69,70].

The equiatomic CrCoNi medium entropy alloy (MEA) shares similarities with HEA in its exceptional mechanical properties, such as high tensile strength, excellent work-hardening rate, and remarkable fracture toughness. In a recent study, MEA CrCoNi particles have been utilized to reinforce ceramic matrix composites (CMCs) featuring a micro-laminated structure [71]. The investigation focuses on understanding how the microstructure contributes to enhance mechanical properties of the material. The fabricated composites exhibit greater strength compared to pure Cu counterparts. Specifically, incorporating 10 vol.% CrCoNi particles results in achieving high strength ((326±3.9) MPa) and good ductility ((20.9±2.3)%). This improvement could be attributed to several factors: the uniform dispersion of CrCoNi particles throughout the matrix, effective bonding at the interfaces, and the presence of a microlaminated structure. The primary strengthening mechanism identified in these composites is load transfer strengthening. Analysis of the interface between CrCoNi particles and the Cu matrix (Fig. 8) reveals predominantly sharp interfaces, indicated by the green line. Importantly, minimal interfacial diffusion or reaction is observed, which is advantageous for reducing potential interface contamination and maintaining composite integrity.

3 Micro-composite copper alloy

Micro-composite copper alloys are also known as binary Cu−X composites, and the X elements often have low solid solubility in Cu matrix, such as Nb, Fe, W, Cr, Mo, Ta, V and Ag [72−75]. Upon

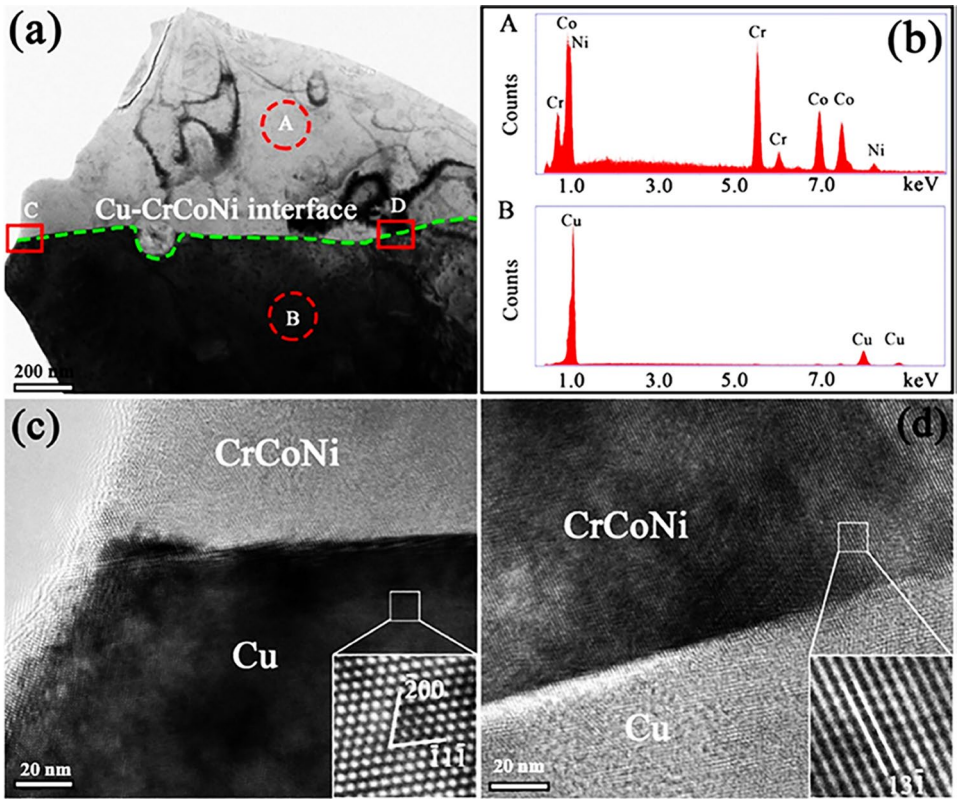

Fig. 8 Interface microstructure for 20 vol.% CrCoNi/Cu composite: (a) BF image; (b) EDS results recorded from Zones A and B marked in (a); (c) HRTEM image of Zone C marked in (a); (d) HRTEM image of Zone D marked in (a) [71]

solidification of these alloys, body-centered cubic (bcc) dendrites form in the copper matrix, and subsequent mechanical deformation reduces the dendrites to aligned filaments with a ribbon-like cross-section. The limited solubility of these bcc metals in copper ensures that the matrix retains a high conductivity, making these in-situ composite for applications where high conductivity and high strength are required. In this chapter, the research status of several kinds of typical composites that are Cu−Nb, Cu−Fe, Cu−Ag, Cu−Cr and Cu−W is introduced emphatically.

3.1 Cu−Nb composites

Cu−Nb composites are considered a crucial material for non-destructive high-field pulse magnets due to their advantages of high strength, excellent thermal conductivity and electric conductivity, which have a broad application prospect in the high-intensity magnetic field [76,77]. However, it is hard to compound them evenly through melting, on account of the melting points of Cu and Nb differing by about 1400 °C. The preparation methods of Cu−Nb composites are mainly divided into in-situ deformation composite and mechanical alloying. The mechanical properties of deformed composites Cu−Nb are shown in Table 5 [78−85]. The strength of the deformed composites Cu−Nb increases with the increase of Nb content. High Nb content in Cu−Nb alloy is not conducive to the subsequent processing and reduces the electrical conductivity of the alloy.

Although Cu and Nb are almost immiscible with each other, they can also be transformed into supersaturated solid solutions by the mechanical alloying (MA) method. Subsequent processing allows for the preparation of high-strength nano-dispersion strengthened copper alloys by precipitating Nb particles. In addition, the composition of the alloy can be continuously adjusted. In the study of solid solutions, Cu−Nb composites were prepared using the MA method [85]. It has been reported that Cu90Nb10 powders achieve Nb dissolution in the Cu matrix after prolonged milling, where a single-phase supersaturated solid solution of Nb in Cu with Nb content ≥15 wt.% is obtained [86]. Furthermore, severe plastic deformation techniques, including traditional drawing, accumulative bundling and drawing (ABD), and accumulative roll bonding (ARB), have been employed to produce high-strength and high-conductivity Cu−Nb composites [86]. Studies show that through multiple extrusion and drawing cycles, a ⟨111⟩ orientation texture can be developed in the Cu matrix, while the Nb core exhibits a ⟨110⟩ deformation texture aligned parallel to the tensile axis. After heat treatment, changes in the crystal plane orientations of the Cu−Nb material can be observed, with a slight increase in the intensity of Cu (111) and Nb (110) peaks, indicating a recrystallization process.

To address the trade-off between mechanical and electrical properties, extensive research has focused on copper and its composites with nanostructures to enhance strength without significantly compromising electrical conductivity [87]. Cu/Nb multilayer composites fabricated using accumulative roll bonding (ARB) techniques have been particularly successful. These composites exhibit ultrahigh tensile strengths (~1.2 GPa) while maintaining excellent electrical conductivity, effectively overcoming the typical trade-off between strength and electrical properties. The formation of nano-laminate Cu/Nb composites with a preferred ⟨111⟩Cu//⟨110⟩Nb//RD orientation has been revealed through analysis combining diffraction pattern indexing with morphology (Fig. 9(a)) [88]. The results confirm the relationship of predominant rolling textures: {220}⟨111⟩Cu and {110}⟨110⟩Nb (in the {TD}⟨RD⟩ notation) in the nano-laminated Cu/Nb composites after 14 ARB cycles. Inverse FFT (IFFT) images of the atomic structure at the interface show a regular array of edge dislocations (Fig. 9(d), marked as "T" symbols [89]). This semi-coherent interface structure with edge dislocations

Table 5 Mechanical properties of deformed composites Cu−Nb at room temperature [78−85]

Fabrication	Composition	Yield strength/ MPa	Ultimate stress/ MPa
In-situ compositing	Cu−5.5vol.%Nb	584	822
	Cu−7.4vol.%Nb	706	938
	Cu−9.2vol.%Nb	799	1068
	Cu−12.5vol.%Nb	867	1211
	Cu−18vol.%Nb	−	1530
Non-in-situ compositing	Cu−8vol.%Nb	−	760
	Cu−18vol.%Nb	−	1350

compensates for the lattice spacing mismatch (~0.25 Å) between {111}Cu and {110}Nb planes, effectively hindering dislocation transmission and thereby enhancing the strength of materials.

3.2 Cu−Fe composites

Cu−Fe composites have many potential advantages including rich raw materials, low cost, easy melting, considerable magnetoresistance effect and good deformation ability. They can be used as magnetic conducting, electromagnetic shielding, discharge machining materials and so on [90]. A comparison of conductivity and tensile strength of Cu−*x*Fe composites fabricated by the in-situ deformation is presented in Table 6 [90−95]. It can be obtained that the strength of composites increases with the increase of Fe content and the deformation rate in Cu−Fe composites. The contradiction between high strength and high conductivity always exists for Cu−Fe composites [96]. The increase in alloy strength could inevitably lead to a decrease in conductivity.

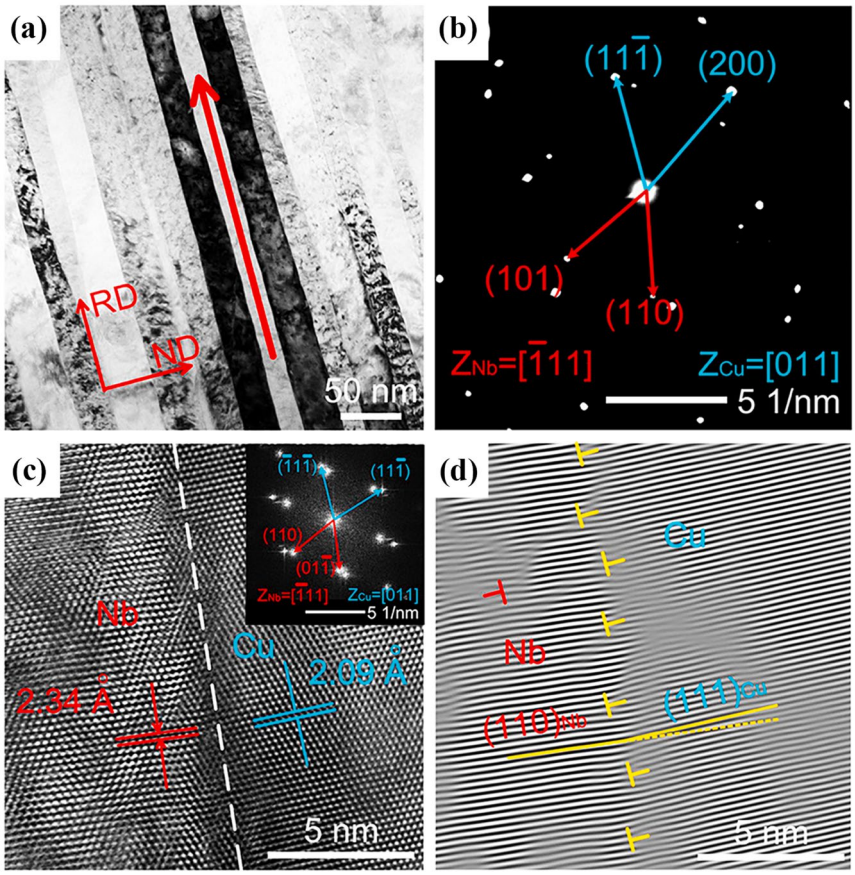

Fig. 9 (a) Cross-sectional TEM images of Cu/Nb nanolaminate composites after processing by ARB through 14 cycles; (b) Corresponding SAED pattern of (a); (c) HRTEM image of Cu/Nb interface from (a); (d) IFFT image of (c) exhibiting distribution of misfit dislocations near interface [88]

Table 6 Electrical conductivity and tensile strength of Cu−*x*Fe composites prepared by in-suit deformation

Composition/wt.%	Processing method	Drawing strain	σ_b/MPa	Electrical conductivity/%(IACS)	Ref.
Cu−11.5Fe	Cold-drawing	5.37	659	−	[90]
Cu−12Fe	Cold-drawing	7.6	962	61.6	[95]
Cu−14Fe	Cold-drawing	7.8	790	52	[91]
Cu−15Fe	Cold-drawing	6	1200	47.6	[92]
Cu−20Fe	High-pressure torsioning (HPT)	6 (HPT strain)	700	−	[93]
Cu−20Fe	Cold-drawing	9.2	950	69	[94]
Cu−30Fe		9.2	1310	55	[94]

Cu−Fe alloys have positive mixing enthalpy and meta-stable miscibility gaps, leading to liquid-phase separation between Cu and Fe during solidification [97]. This is a bottleneck that limits the preparation and engineering application of high-performance Cu−Fe alloys. The main challenges to obtain high-quality Cu−Fe alloy billets through casting methods are to overcome the separation of Fe-rich and Cu-rich liquid phases during solidification and suppress the severe macro-segregation of the Fe phase. Currently, the reported preparation methods for Cu−Fe composites mainly include deformation composite methods, powder metallurgy, multi-alloying, rapid solidification, and other special casting techniques [98]. The in-situ deformation method is the most extensively studied, typically involving casting followed by subsequent deformation processes. In the initially prepared Cu−Fe composites by the powder metallurgy and casting, Fe dendrites that form in the Cu matrix gradually evolve into aligned fibres during subsequent extrusion, swaging, or drawing processes.

The powder metallurgy method can avoid the issue of component inhomogeneity caused by the physical and chemical differences and the solubility differences of various elements. This is particularly effective in the preparation of Cu−Fe composites, as it can effectively avoid the structural segregation caused by the liquid-phase separation during casting [99]. Additionally, changing the sintering parameters can control the content of Fe atoms in the Cu matrix, reducing the adverse effects on the electrical conductivity of the composites. WANG et al [92] have found that Cu−Fe alloys using a pre-alloyed powder method achieve the average size of primary Fe phase of 1.0−2.8 μm, which is much smaller than that of cast Cu−Fe alloys (20−30 μm). After deformation with a strain rate ($\dot{\varepsilon}$) of 5.0, a strength of 1150 MPa and electrical conductivity of 52%(IACS) can be obtained in their study.

Current work on the rapid solidification of Cu−Fe alloys mainly focuses on the microstructural refinement and the mechanism of liquid-phase separation. GUO et al [100] have reported the solidification microstructure of rapidly solidified Cu−Fe−C alloys at different cooling rates. At the cooling rates of 0.515×10^3−0.773×10^4 K/s, the dual-scale (2−3 μm and 100 nm) FCC Fe−C phases are uniformly distributed in the matrix. After 95% room temperature rolling, the tensile strength of the composite reaches 511 MPa [100]. JO et al [97] have found that the strength of Cu−10Fe−2Si alloys prepared by the spray casting method reaches 635 MPa. The average size of α-Fe particles in the solidified microstructure of Cu−10Fe−2Si alloys is 0.76 μm. Given that the primary cause of Fe phase segregation is the formation of Fe-rich liquid (L1) and Cu-rich liquid (L2) during solidification [101], with density difference causing macroscopic segregation under gravity, a new double melt mixing casting process could be developed to prepare large Cu−Fe alloy billets with fine microstructure and uniform Fe phase distribution. This process involves combining pure copper and Cu−Fe master alloy, utilizing electromagnetic stirring and rapid solidification techniques. These methods effectively suppress macro-segregation of the Fe phase and precisely control the size and distribution of Fe particles during solidification. Subsequent cold deformation and multi-stage deformation heat treatment further refine the microstructure of the composites and control the size, distribution, and orientation of the Fe phase. The Cu−10wt.%Fe alloy prepared using this process shows primarily dendritic and spherical Fe phases, uniformly distributed within the matrix, with sizes ranging from 5 to 20 μm (Fig. 10).

To achieve an excellent combination of strength and conductivity in Cu−Fe composites, it is essential to suppress the solid solution of Fe in the Cu matrix and promote the precipitation of the Fe phase. Therefore, various alloying and heat treatment methods have been employed in experimental studies on this topic. Intermediate heat treatment can improve dendrite distribution and promote secondary precipitation of Fe [102]. However, heat treatment alone cannot completely inhibit the solid solution of Fe, and prolonging heat treatment often causes the Fe fibres to coarsen, leading to a rapid decrease in material strength. Therefore, selecting different alloying elements according to specific research goals to achieve different mechanical and electrical properties is crucial. Numerous studies have also focused on developing ternary Cu−Fe−X systems (X=Mg, Ag, Co, Si, Nb, or rare-earth elements) [96,97,102−105]. The addition of Mg significantly increases the tensile strength of Cu−Fe alloys by refining the Fe

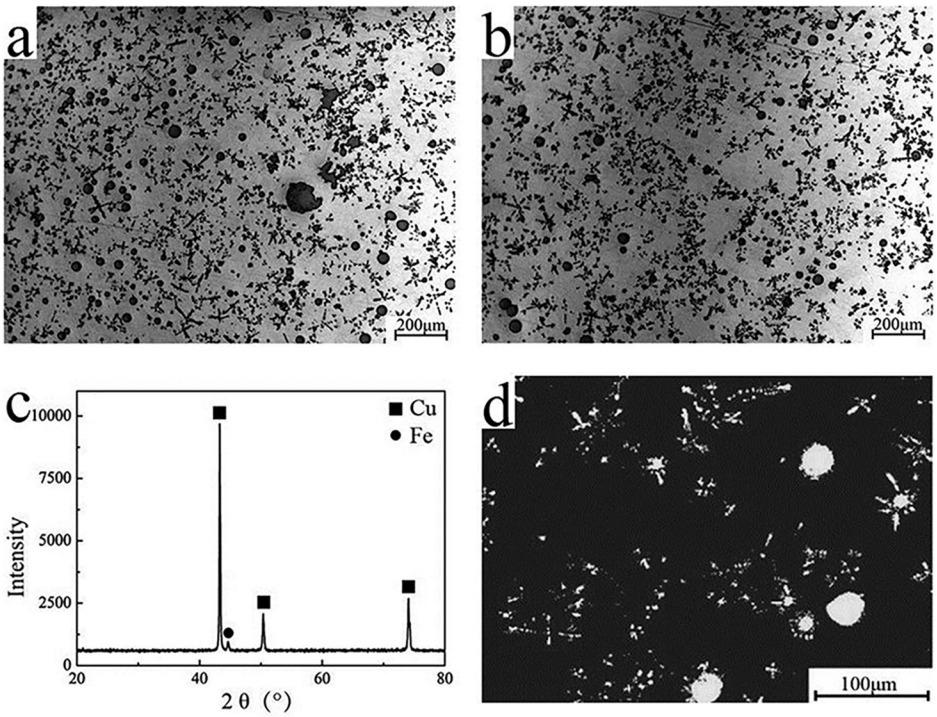

Fig. 10 Microstructure of as-cast Cu−10wt.%Fe alloy prepared by double melt mixed casting: (a) Top of ingot; (b) Bottom of ingot; (c) XRD pattern; (d) Phase distribution of EBSD [101]

phase and reducing dendritic segregation, although it slightly reduces the electrical conductivity of the composites [103]. Adding Ag into Cu−Fe composites can effectively improve their electrical conductivity and mechanical properties [96,105]. Ag atoms in solution increase the lattice constant of the Cu matrix, accelerating the diffusion rate of Fe atoms and promoting the precipitation and nucleation of γ-Fe. The addition of Nb in Cu−Fe composites can promote the heterogeneous nucleation of γ-Fe by in situ forming Fe_2Nb, thereby refining the primary Fe phase [74]. In prior studies, it is observed that rolled Cu−Fe composites at lower temperatures successfully suppress dynamic recrystallization within the Cu matrix during deformation. This approach substantially boosts the work-hardening effect, leading to marked improvements in the mechanical performance of composite [102]. Moreover, the application of rapid cooling led to the emergence of numerous nanoscale Fe phases distributed throughout the Cu−Fe matrix [106]. These nanoscale Fe phases serve as anchoring points for dislocations formed during subsequent deformation, which further hinders dynamic recrystallization in the Cu matrix. Consequently, lowering the deformation temperature and increasing the presence of nanoscale phases in the matrix are critical strategies for enhancing the strength of Cu−Fe composites during deformation.

3.3 Cu−Ag composites

Copper and silver are highly conductive materials, but both pure copper and pure silver have lower strength. For Cu−Ag composites, Ag exhibits less influence on the conductivity of copper alloys than other alloying elements and it can enhance the strength of the matrix as well [107]. The research and development of Cu−Ag alloy are mainly to meet the needs of high pulsed magnetic field conductor materials. Cu−Ag alloy, as one of the excellent conductive materials, can also be used in many fields such as aerospace rail transportation machinery manufacturing and large-scale integrated circuits [107−109]. The conductivity and tensile strength of Cu−Ag composites with different deformation rates are listed in Table 7 [107−113]. With the increasing Ag content, the strength of Cu−Ag increases rapidly; however, when Ag content is greater than 10%, the strength of Cu−Ag gradually saturates and reaches the maximum when the Ag content is a eutectic component [107].

Table 7 Electrical conductivity and tensile strength of Cu−Ag composites with different drawing stain

Composition/wt.%	Processing method	Drawing strain	σ_b/MPa	Electrical conductivity/%(IACS)	Ref.
Cu−3.5Ag	As-cast	0	−	86.2	[108]
Cu−4Ag	Cold-drawing	9	−	77	[109]
Cu−4Ag	Cold-drawing	11.28	1048	75.2	[107]
Cu−6Ag	Cold-drawing	7	1150	75	[112]
Cu−12Ag	Cold-drawing	7	1300	65	[112]
Cu−7.9Ag	Cold-rolling	3.7	888	−	[110]
Cu−10Ag	Cold-drawing	10	1550	65	[113]
Cu−26Ag	Cold-rolling	7.4	844	−	[111]

The microstructure of Cu−Ag alloy with a high content of Ag is difficult to control by the traditional melting-casting method, requiring a series of heat treatments to eliminate the composition segregation. The application of the directional solidification preparation method in Cu−Ag alloys could also be a promising technology. The as-cast Cu−Ag alloys prepared by directional solidification did not require complicated intermediate annealing due to the high cooling rate, reducing the energy consumption and shortening the preparation process significantly. The drawing process can be divided into three stages: general deformation, large deformation, and extreme deformation. The primary deformation mechanisms of each stage include dislocation slip and twinning, dynamic recovery and layered interface evolution, and partial dynamic recrystallization. The increased strain raises the storage energy of the alloy, forming deformation twins locally. At a strain of 3.41, numerous sub-structures and recrystallizations are evenly distributed in the alloy, accounting for 35.1% and 4.1%, respectively [107]. Increased dislocation entanglement often causes severe local stress concentration, enhancing shear deformation and converting matrix bands to sub-bands (Fig. 11(a)). A few sub-grains usually form due to the cross-slip mechanism (Fig. 11(b)). Additionally, many stacking faults and nano-twins are often found in the Ag phase (Fig. 11(c)).

To improve the performance and reduce production costs, the strength of Cu−Ag alloy can be obtained by adding third elements such as Nb, Cr, Zr, Fe, and rare earth elements [110,111,114−116]. It has been reported that Nb addition not only strengthens the Cu matrix but also enhances the effect of Ag precipitates through a synergistic effect on the ratio of coherent precipitates (CPs) to dispersed precipitates (DPs) [110]. The addition of 0.1 wt.% Fe to the Cu−26wt.%Ag alloy refines the morphology of the eutectic structure and Ag precipitates [111]. Fe precipitates introduce the strain fields around the Ag precipitates, forming overlapping elastic strain fields. These strain fields control the soft impingement diffusion of Ag and inhibit the nucleation of Ag precipitates, resulting in smaller Ag precipitates in the Cu−26Ag−0.1Fe alloy compared to those in the Cu−26Ag alloy.

3.4 Cu−Cr composites

Cr is a promising reinforcing metal for Cu-based in situ composites due to the relatively economical cost, limited solubility in Cu and high tensile strength [117]. Cu−Cr composites with high Cr content have many applications in electrical industries such as integrated circuit lead frames, electric resistance welding electrodes and electric contacts because they exhibit a combination of high mechanical strength with good electrical conductivities [118−120]. According to the Cu−Cr binary diagram, when the content of Cr is between 1.7% and 40%, the typical microstructures of as-cast samples consist of bcc Cr-rich dendrites distributed in Cu-rich matrix. Cu−Cr alloys produced by traditional melting and casting processes usually possess coarse Cr dendrites. Because the solid solubility between Cu and Cr is very low, thermal or mechanical treatments have limited effect on improving this microstructure. To achieve fine Cr in phase, many new techniques such as melt spinning [121], mechanical alloying

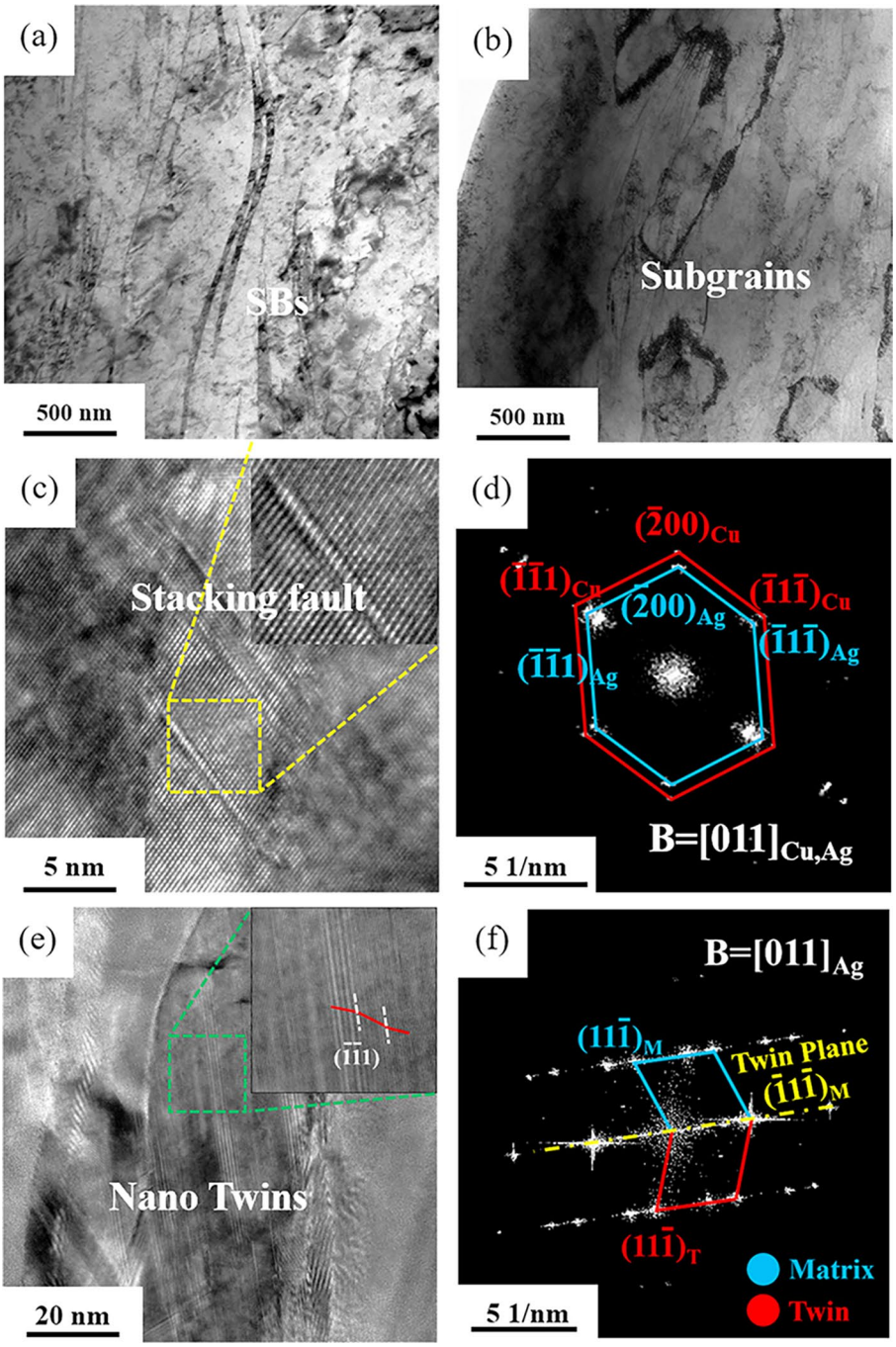

Fig. 11 TEM images of Cu−4wt.%Ag alloy at drawing strain of 3.41: (a, b) BF image; (c, e) HRTEM image; (d, f) SAED patterns of (c) and (e), respectively [107]

electromagnetic levitation and splat-quenching have been applied to preparing Cu−Cr alloys. However, these techniques are usually complicated and uneconomical. The addition of the third element can enhance the comprehensive properties of such materials. To date, ternary alloying elements such as Zr, Ag, Co and rare earth have been applied to developing novel Cu−Cr alloys. The conductivity and tensile strength of Cu−Cr composites with or without dropping ternary alloying elements are listed in Table 8 [116,119,120−124]. It is clear that with the addition of the elements mentioned above, the tensile strength of Cu−Cr alloy has been improved to some extent, with negligible effect of conductivity.

The impact of Ag micro-alloying on Cu−7Cr in situ composites has been investigated by comparing the Cu−7Cr and Cu−7Cr−0.07Ag

composites [123]. The Cu−7Cr−0.07Ag composites exhibit higher ductility and conductivity than Cu−7Cr. The addition of trace Ag refines the microstructure of Cu−7Cr in situ composites by enhancing the interaction among Ag, Cu and Cr, facilitating the formation of a Cu solid solution and decreasing the solubility of Ag and Cr in the Cu matrix. The effects of adding 0.4 wt.% Zr to Cu−10Cr composites show that Cu−10Cr−0.4Zr composites exhibit smaller as-cast Cr dendrites, resulting in finer filaments at higher strains compared to base Cu−10Cr composites [116]. At a draw ratio of 6.2, Cu−10Cr−0.4Zr composites achieve an ultimate strength of 1089 MPa, whereas Cu−10Cr composites only have a strength of 887 MPa in the same conditions [116]. The enhanced strength of Cu−10Cr−0.4Zr in situ composites is mainly attributed to the Hall−Petch strengthening from closely spaced Cr filaments, the reinforcing effect of Zr, and a strengthened Cu matrix. Usually, Zr addition can lead to the formation of a thin CuZr compound phase in Cu−15Cr alloys, and Zr inhibits the formation of eutectic Cr, resulting in significantly reduced eutectic Cr content compared to Cu−15Cr alloy [119]. In Cu−15Cr alloy, eutectic Cr surrounds dendritic Cr extensively, whereas, in Cu−15Cr−0.24Zr alloy, eutectic Cr content is lower and distributed in a bar-like dispersion within the Cu matrix, as shown in Fig. 12.

3.5 Cu−W composites

Cu−W system composites have essential applications due to their superior physical and mechanical properties, such as low thermal expansion coefficient, high melting point and high strength. W is a material with high heat resistance, high hardness, and low thermal expansion coefficient [125−127]. Because Cu and W are not mutually soluble and have poor wettability with each other, they can only form a pseudo-alloy called Cu−W by alloying mechanically [128]. The thermal, electrical and mechanical properties of Cu−W composites can be controlled by changing the content of W in the Cu matrix. Therefore, the content of Cu and W is regulated according to the specific use conditions, so Cu−W composites have been widely used in fields of electrical, electronic field, high-temperature, military and other aspects [129,130]. In order to obtain a matching coefficient of thermal expansion, the content of Cu in Cu−W composites for electronic packaging is generally less than 20 wt.%.

The Cu−W composite material can be used at high temperatures through the gasification of vast heat absorption to reduce the surface temperature of the material, so the high-temperature Cu−W composite is generally used with Cu−(5−10)wt.%W composite. To obtain better Cu−W composites, the improvement of the properties of Cu−W composites is mainly concentrated in two aspects. The first is to improve the preparation process of Cu−W composites, and the second is to improve the properties of Cu−W composites by adding the third phase. At present, the traditional preparation methods of Cu−W composites mainly include: (1) high-temperature liquid phase sintering method; (2) activated liquid phase sintering method; (3) solution infiltration method; (4) mechanical alloying method. High density is a prerequisite for Cu−W composites with excellent properties. However, because Cu−W is not mutually soluble, dense Cu−W composites are often prepared by powder metallurgy.

Table 8 Electrical conductivity and tensile strength of Cu−Cr composites

Composition/wt.%	Processing method	σ_b/MPa	Electrical conductivity/%(IACS)	Ref.
Cu−1Cr	Hot-rolling	−	68	[122]
Cu−1Cr−5CNT	Hot-rolling	−	62	[122]
Cu−7Cr−0.07Ag	Cold-drawing	772	77.3	[123]
Cu−10Cr	Cold-drawing	887	36.1	[116]
Cu−10Cr−0.4Zr	Cold-drawing	1089	35.2	[116]
Cu−3.11Cr	Rotary swaging	575	70	[124]
Cu−15Cr−0.24Zr	Cold-drawing	1023	72	[119]

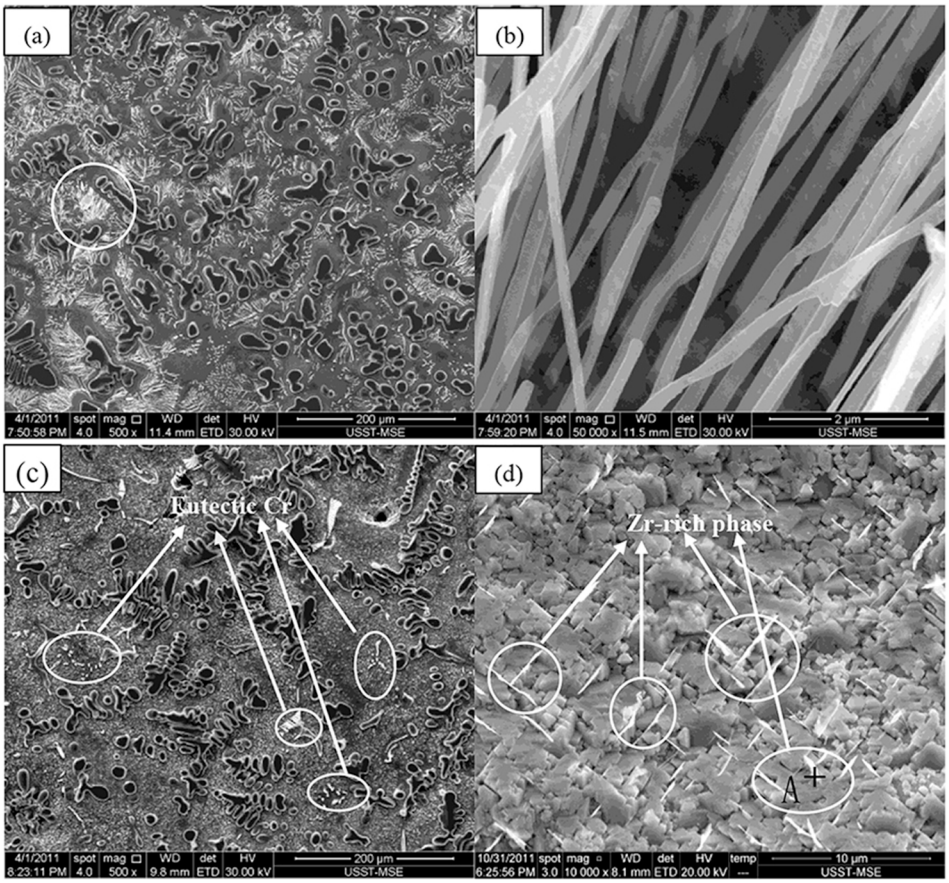

Fig. 12 SEM images of as-cast alloys after corrosion: (a) Cu−15Cr alloy; (b) Eutectic Cr in selected region of (a); (c) Cu−15Cr−0.24Zr alloy; (d) Zr-rich phase in Cu matrix [119]

Researchers have advanced the development of 20wt.%Cu−W composites with exceptional properties by employing an electroless plating technique to deposit a dense Cu layer on the surface of W particles, followed by hot pressing. Under conditions of 95 °C and 100 MPa for 2 h, the resulting composite achieves a density exceeding 97% and a thermal conductivity of 239.0 W/(m·K), closely approaching the theoretical value for 20wt.%Cu−W composites [131]. This methodology significantly outperforms the traditional mixing techniques in terms of enhancing thermal conductivity. Additionally, Cu−W alloys subjected to high-current pulsed electron beam (HCPEB) irradiation have been investigated, with marked improvements in surface microhardness through HCPEB [132]. The irradiation process induces the formation of Cu(W) solid solutions, the development of ultrafine grains, the generation of amorphous phases, and the emergence of long-period superlattice phases. Transmission electron microscopy (TEM) analysis of samples irradiated up to 10 pulses reveals the presence of three distinct types of W particles within the modified layer.

The related studies demonstrate that nanoscale W-coated Cu−Cu−W composite powders have been initially prepared using spray drying followed by a two-step hydrogen reduction method [133]. Cu−W composite materials are fabricated via spark plasma sintering (SPS), which significantly enhances their mechanical properties while maintaining the excellent electrical conductivity of the Cu matrix. The W-coated Cu−Cu−W composite powders effectively inhibit the growth of Cu grains during sintering, leading to refined Cu grain sizes. Additionally, a good interfacial bonding between Cu and W is characterized by a semi-coherent relationship between Cu(111) and W(110) as shown in Fig. 13.

Cu−W films are widely used for protection, decoration and diffusion resistance. Cu−W films also have the advantages of high hardness, high strength, low expansion coefficient and excellent electrical conductivity. Recently, the research on

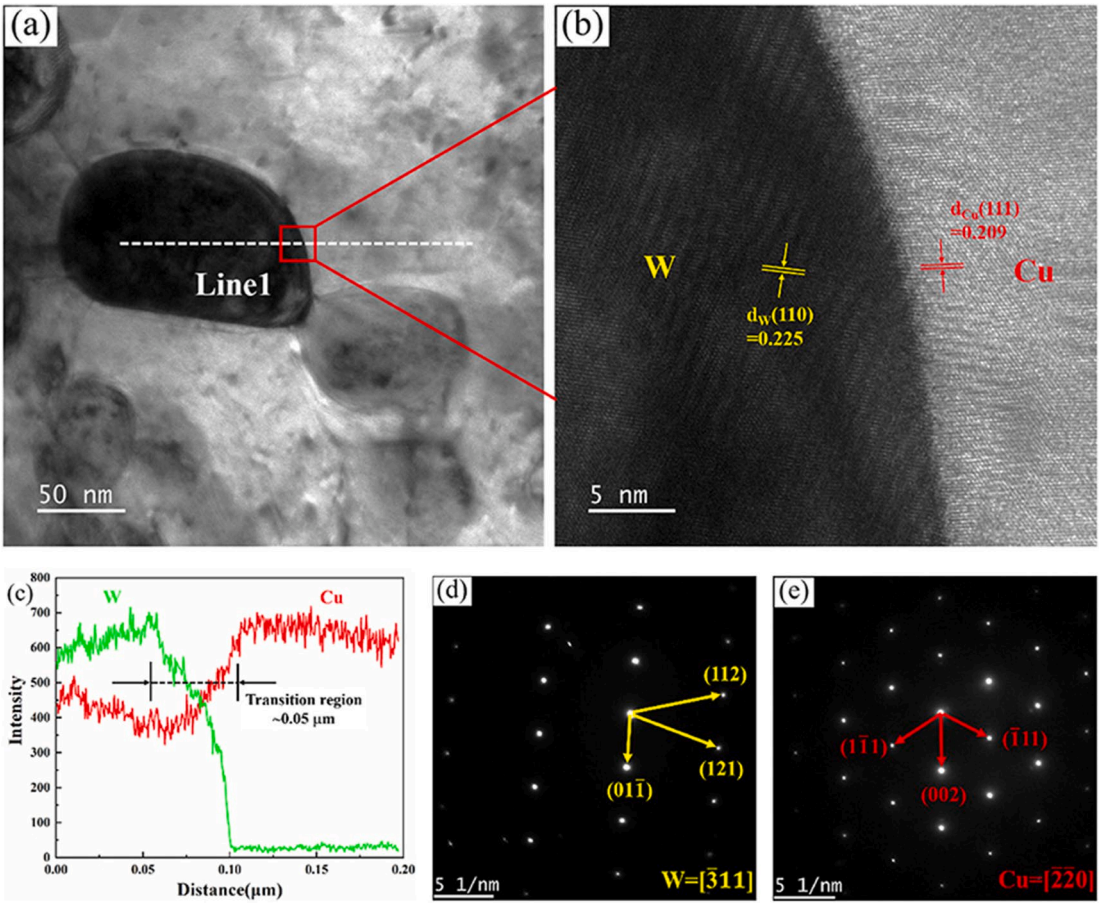

Fig. 13 (a) TEM micrograph of Cu−20W composite; (b) HRTEM micrograph of red box area in (a); (c) Line scan EDX analysis of Line 1 in (a); (d) SAED pattern of black interface in (b); (e) SAED pattern of white interface in (b) [133]

Cu−W films mostly focuses on the multilayer composite films that form under extreme conditions, such as Cu−W multilayer films deposited by magnetron sputtering, ion beam sputtering, ion beam irradiation and electron beam evaporation. A series of Cu−W films with W content exceeding 17.2 at.% can be prepared using magnetron sputtering-focused co-deposition technology [134]. The variation in microstructure and hardness with the increasing W content has been investigated. The films exhibit phases including FCC, amorphous, and bcc within their multilayered structure. The high-density interfaces within the multilayers effectively inhibit dislocation movement, resulting in hardness levels at least 2 GPa higher than that predicted by the mixing rule. In Fig. 14(a), a HAADF-STEM image of a Cu−62at.%W film shows prominent columnar and multilayered structures. HR TEM images further reveal the coherent or semi-coherent nature of interfaces between Cu-rich and W-rich layers. Similarly, according to the TEM image of Cu−80at.%W films, the multilayered structure persists but becomes increasingly distorted and discontinuous due to the significant cracks and porosity among the pronounced columnar structures. Figure 14(d) illustrates that in Cu−26.3at.%W films, the multilayered structure remains present, although with less distinct and more disorderly interfaces between Cu-rich and W-rich layers. Additionally, the amorphous and nanocrystalline phases with bcc and FCC structures are often found in the composites.

4 Cu−carbon composites

Cu−carbon composites are as a new type of functional material which is made of copper matrix and C materials. Typically, C materials include graphite, carbon nanotubes, carbon fibre and graphene, etc. Cu−carbon composites exhibit the characteristics of both Cu and C materials, possessing both the high electrical and thermal conductivity properties of Cu and the self-lubricating properties of C materials. Therefore,

they are widely applied in the mechanical transportation, aerospace and other fields with special electrical conductivity requirements and wear resistance [135,136], as listed in Table 9.

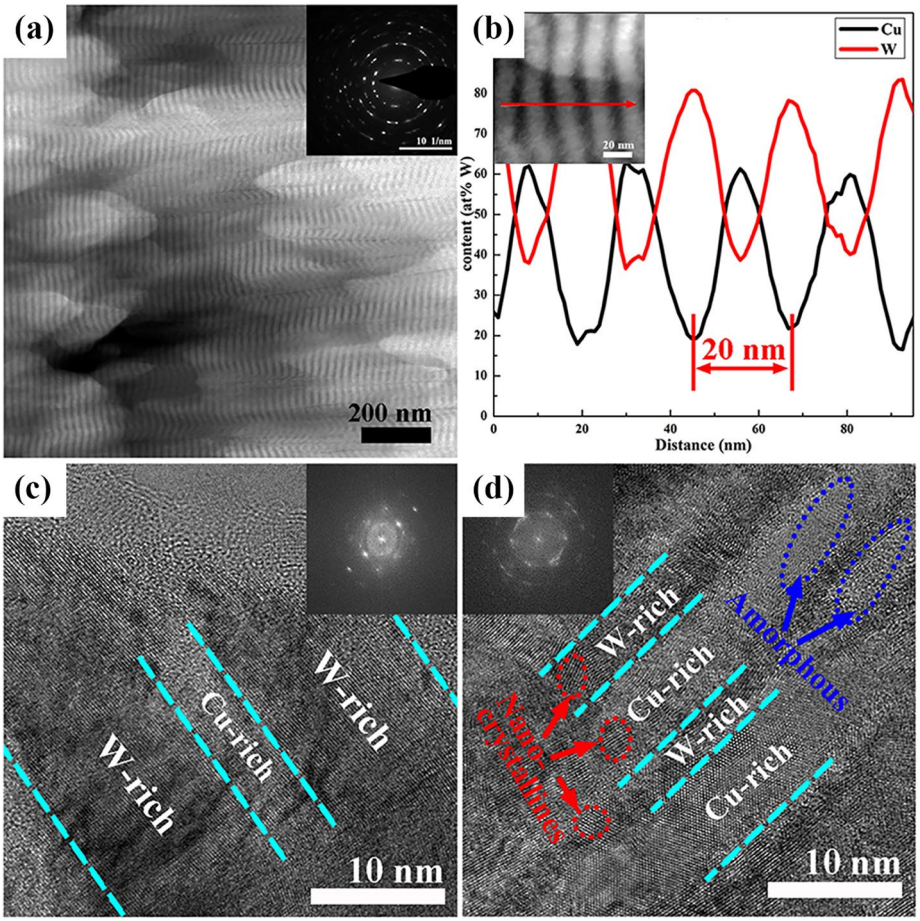

Fig. 14 TEM analysis of cross-sectional morphologies of Cu−W films with different compositions: (a) HAADF-STEM; (b) Line scanning; (c) HRTEM image of Cu−62at.%W film; (d) HRTEM image of Cu−26.3at.%W film [134]

Table 9 Functional characteristics and applications of Cu−carbon composites [137−139]

Type of material	Structure of C-material	Functional characteristics of Cu-carbon composite	Application of Cu-carbon composite
Graphite	Lamellar structure	Excellent electrical conductivity, wear resistance, lubrication effect and arc resistance erosional characteristic.	The preparation of electronic packaging, brush materials sliding contact materials, pantograph sliding plate materials, self-lubricating materials and other fields.
Carbon-nanotubes	Topological nanotubes structure	High strength, high electrical conductivity, high thermal conductivity and high wear resistance	The field of electromagnetic shielding in aerospace. It is often used as a material for large-scale integrated circuits, electronic radar and pulsed magnetic field conductors.
Carbon-fiber	Fibre	Excellent mechanical properties and chemical stability, high tensile strength, high interlaminar shear strength, high Young's modulus, low density, low thermal expansion, and good electrical and thermal conductivity.	Instead of Ag, W, Mo and other expensive and difficult-to-process traditional metal materials to produce semiconductor support electrodes and contact materials.
Graphene	Honeycomb lattice	Load transfer enhancement of Orowan enhancement of fine grain enhancement and thermal mismatch enhancement.	The fields of supercapacitor ion battery and biosensing.

4.1 Cu−graphite composites

In recent years, the types of reinforcing phases, strengthening methods and preparation technology of Cu−C composites have changed constantly. By controlling the structure, content and spatial distribution of C materials in the Cu matrix, CMCs with excellent mechanical properties, functional properties, chemical stability and compatibility can be obtained [140,141]. Graphite has attracted much attention for its excellent electrical and thermal conductivity, self-lubricating properties, and moderate wear resistance, making it an ideal solid lubricant. Consequently, graphite-reinforced Cu-based composites are developed using the benefits of both Cu and graphite, satisfying the performance criteria required for new sliding materials, such as high electrical conductivity, outstanding wear resistance, and superior lubrication properties.

However, the poor wettability between graphite and Cu results in weak mechanical bonding at the matrix−reinforcement interface, significantly restricting the application of graphite/Cu composites. Enhancing the interfacial wettability between graphite and Cu is therefore a critical focus for researchers. Studies have shown that chemical plating on the graphite surface (e.g., Ag, Cu) is an effective approach to improve its interfacial bonding with Cu [142−144]. Moreover, researchers have pioneered a novel approach to fabricating high-quality copper−graphite composites using cuprous oxide in place of copper and graphite through an in situ reaction method [145]. The composites produced demonstrate a hardness increase of 1.5 to 1.6 times compared to the original material, with a corresponding rise in compressive strength by 50−100 MPa. The in-situ reaction occurs at specific temperatures and involves a redox process at the interface between cuprous oxide and graphite particles ($2Cu_2O(s) + C(graphite) \rightarrow 4Cu(s) + CO_2(g)$). Although the interfacial bonding in Cu_2O−Gr is strong, the electrical resistivity of Cu_2O−Gr and Cu−Gr composites remains similar, showing that the in-situ reaction has a minimal effect on improving electrical conductivity. Research also indicates that using nearly spherical graphite powder of consistent size can enhance the composite's density and mechanical properties, boosting compressive strength by around 65 MPa [146].

4.2 Cu−CNTs composites

CNTs−Cu composites are recognized for their superior mechanical properties, electrical and thermal conductivity, and tribological performance, making them promising materials for electrical contacts, electrical packaging, and heat exchange applications [147]. CNTs are favorable due to their exceptionally high strength, electrical conductivity, high capacity, and low density, which are attributed to their robust C═C bonds and extensive π-conjugation [148,149]. Research shows that at room temperature, CNT−Cu composite wires exhibit enhanced electrical performance and capacity compared to pristine carbon nanotube fibres [150−154]. Achieving uniform dispersion of CNTs within the matrix is a primary objective, with special fabrication methods such as high-energy ball milling, in situ chemical vapour deposition, and friction stir processing being employed [155,156]. However, the poor wettability and weak interfacial interactions between CNTs and the Cu matrix still result in a significant reduction in the mechanical properties of CNT−Cu wires [157].

To address this problem, elements like Al, Nb, Ti, Cr, and Ni are added to facilitate solid-phase reactions that form stable carbides, thereby enhancing interfacial affinity and promoting the formation of chemical bonds between CNTs and Cu [158,159]. Prior studies have demonstrated that introducing a continuous Ni buffer layer before Cu deposition can create a strong CNT−Cu interface, which aids in Cu deposition and results in superior electrical and mechanical properties [158]. Additionally, optimizing the internal structure and properties of CNT fibres is essential for achieving outstanding performance in CNT−Cu composite fibres. Reports indicate that densification of CNT fibres using chlorosulfonic acid (CSA) is one of the most effective methods for regulating the microstructure of CNTs, leading to the improvement of strength and capacity of CNT/Cu composite fibres when combined with Ni_{DPL} pre-seeding before Cu plating [160]. As shown in Fig. 15, Ni_{DPL}, created on CNT fibres through the high-temperature decomposition of nickel acetate, enhances the chemical affinity and promotes the phonon/electron transfer between CNTs and Cu, without forming a continuous Ni buffer layer.

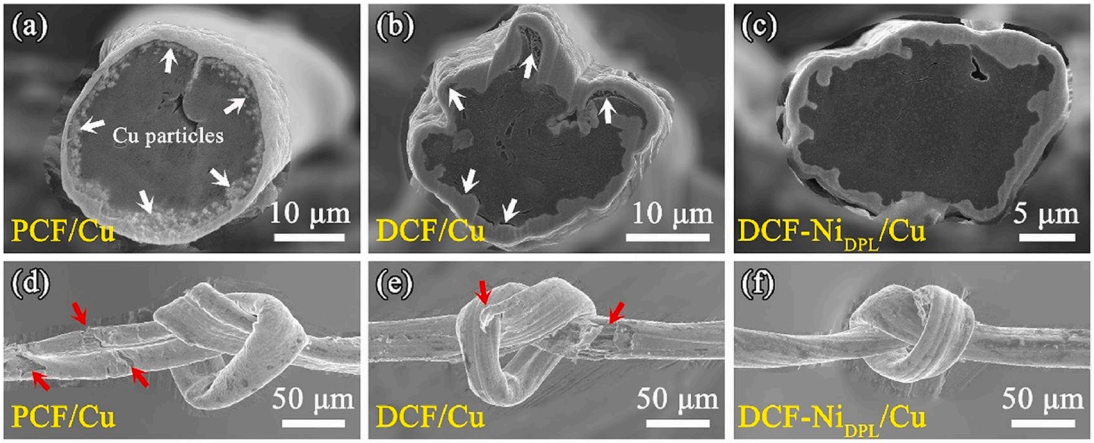

Fig. 15 Cross-section morphology of PCF/Cu (a), DCF/Cu (b), DCF-NiDPL/Cu (c); Surface microstructure of PCF/Cu composite wires (d), DCF/Cu composite wires (e), and DCF-NiDPL/Cu composite wires (f) [160]

4.3 Cu−carbon fibres composites

Carbon fibres (CFs) are characterized by their high strength, high modulus, low thermal expansion coefficient, and low density, making them suitable for enhancing the performance of conductors [141]. CF-reinforced composites have been used for conductive or electromagnetic shielding materials boast features such as lightweight and high strength [161]. Within a Cu matrix, CFs help in load transfer and stress reduction, which is crucial for improving the strength and wear resistance of the composite. Additionally, CFs offer excellent corrosion resistance and self-lubricating properties. Consequently, Cu−CF composites are widely utilized in electronic components, contact materials, sliding materials, and self-lubricating materials. However, the high electrical resistivity of CFs compared to metals limits the electrical conductivity and electromagnetic shielding capabilities of these composites. Hence, enhancing the electrical conductivity of CFs is essential. Metallization is an effective approach to improve the electrical conductivity, wettability, and compatibility of CFs with metal matrices [162,163]. Techniques such as physical vapour deposition, chemical vapour deposition, electroplating, and electroless plating are commonly employed for CF metallization [164]. Metals like silver, copper, nickel, zinc, and platinum can be deposited on CF surfaces [165−168], with copper plating being the most effective method for enhancing CF electrical conductivity [169]. It has been reported to utilize electroplating and electroless plating to modify CFs and fabricate Cu−CF composites, and the results show that the electroless copper coatings adhere better to the CF surface compared to the electroplated copper layer [170]. CF-copper composite wires have been also developed using sputtering and electrodeposition techniques, achieving a strength of 3.27 GPa and electrical conductivity of 4.4×10^5 S/cm, which are approximately 10 times and 75% higher than those of traditional copper wires, respectively [171]. Moreover, the composite wires are lighter, with a density of 70% lower than that of copper, positioning them as promising candidates to replace traditional metal wires in the next-generation electrical applications.

4.4 Cu−graphene composites

Graphene (Gr) is a two-dimensional carbon nanomaterial characterized by low density, high aspect ratio, exceptional specific strength, superior electrical conductivity, and excellent thermal conductivity [137]. Compared to other carbon materials, graphene displays enhanced properties when used as a reinforcement in metal matrices [138]. The graphene-reinforced copper matrix composites (Gr/CMCs) are known for their lightweight nature, outstanding physical properties, and remarkable strength and thermal stability [172]. Despite these advantages, several limitations hinder the application of graphene: (1) very poor wettability between graphene and the copper matrix, (2) agglomeration of graphene nanosheets within the matrix due to their high aspect ratio, and (3) obvious sensitivity to thermal damage. To overcome these challenges, researchers have

explored various improvements, such as surface modification, surface coating treatments, catalytic alloying elements, and optimization of preparation processes [173]. Ball milling is commonly used to break up graphene agglomerates, and mechanical exfoliation can produce few-layer graphene.

Moreover, to achieve a uniform dispersion of Cu−Gr matrix, efforts have been made to enhance the interfacial bonding between graphene and copper through techniques like an electrochemical deposition, ball milling combined with powder metallurgy, molecular-level mixing (MLM), and in-situ synthesis by chemical vapour deposition (CVD) [174]. The reduced graphene oxide (rGO) has been employed in conjunction with MLM to prepare Cu composites, which has shown potential for achieving uniform Gr dispersion within the Cu matrix. However, the process is complex and introduces numerous structural defects during the oxidation−reduction stages, adversely affecting electrical conductivity. Ball milling and powder metallurgy are widely used methods to improve graphene dispersion and provide precise control over composition but often result in structural damage to graphene. In contrast, in-situ growth of graphene on Cu powder using CVD has emerged as a promising method to mitigate graphene agglomeration [175]. When combined with powder metallurgy, this approach can further improve the performance of Cu−Gr composites [176]. Figure 16 demonstrates the in-situ preparation method for Cu−Gr composites [174]. Liquid paraffin is applied to the Cu powder surface, allowing it to diffuse during vacuum hot-press sintering. At elevated temperatures, the paraffin decomposes into carbon due to the catalytic effect of Cu, resulting in graphene primarily located along the grain boundaries (Fig. 17). By optimizing factors such as copper powder particle size, paraffin concentration, sintering temperature, and pressure, a three-dimensional graphene network is uniformly dispersed, addressing the aggregation issue of graphene while preserving its structural integrity and enhancing the interface connectivity between Cu and graphene. This approach enables the in-situ formation of high-quality graphene within the copper matrix. The resulting composite, when combined with cold drawing, exhibits both high strength (516 MPa) and excellent electrical conductivity (94.85% IACS).

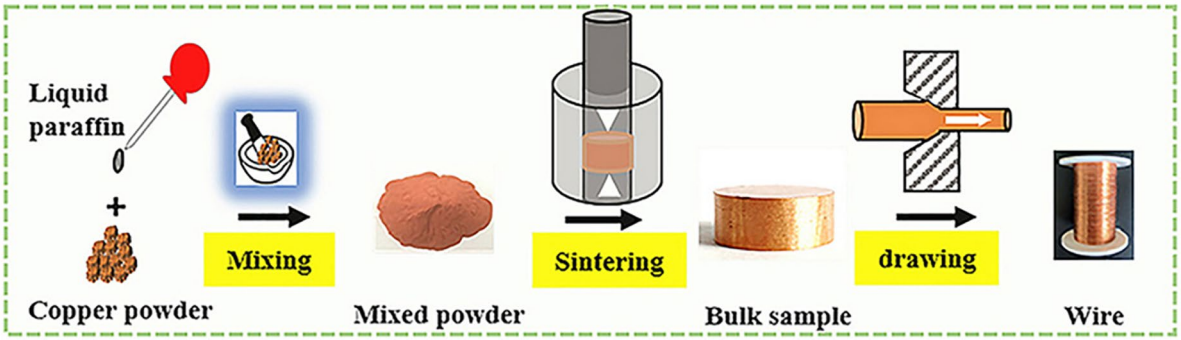

Fig. 16 Schematic diagram of fabrication process of Cu/Gr composite [174]

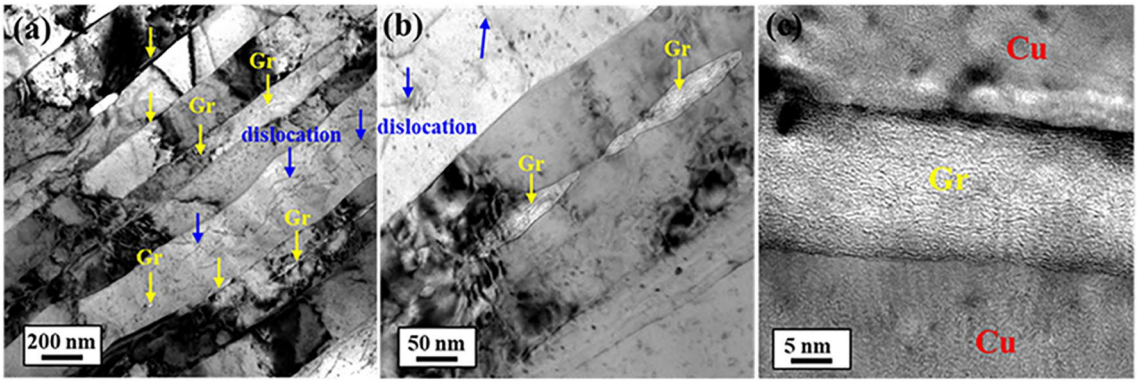

Fig. 17 TEM images of cold drawn Cu/Gr-50 wire: (a, b) BF image; (c) HRTEM image of Cu−Gr interface [174]

5 Conclusions and prospect

CMCs are widely applied to electronics, aerospace, machinery and other areas due to their high specific strength, good wear resistance and corrosion resistance. However, high strength and high conductivity are a pair of contradictory properties for CMCs. The electrical conductivity of composite material is closely related to the matrix and properties, shape, distribution and processing technology of reinforcements. It is necessary to select the appropriate reinforcements, control their volume fraction and shape in material preparation and adjust the processing parameters. Increasing the density of the material and the bonding strength of interface, and reducing porosity and the electron wave scattering can improve the electrical conductivity of the composite material to a certain extent and obtain the CMCs with excellent comprehensive properties such as high conductivity, high strength and high wear resistance. Therefore, it needs to launch further research in the following aspects.

Particle-reinforced CMCs have high strength, high conductivity, good thermal conductivity, high hardness and good wear resistance, and become ideal materials for contact material, spot welding electrode working end, integrated circuit lead frame and casting machine crystallization material, etc. At present, there are many methods to prepare particle-reinforced CMCs. The manufacturing process is relatively complex, and the production cost is still high. Most of the manufacturing processes are limited to the laboratory. The main research direction of CMCs materials is to improve the properties of materials, reduce costs, and achieve industrial production.

With the continuous improvement of the comprehensive properties of the Cu-based alloy, the reduction of the production cost and the advancement of the preparation technology, large-scale industrial production is expected to be realized, and the application prospect is comprehensive. Cu-based alloy can be applied to high pulse magnetic field conductor material, the preferred material for high-speed railway power contact wire, and integrated circuit lead frames, supporting electrodes and aviation propulsion system automatic control cable. The existing research on Cu−Fe deformation in-situ composites shows that Fe fibre is the appropriate strengthening phase in Cu matrix composites with high strength and conductivity. The solid solution Fe atoms in the Cu matrix will seriously damage the conductivity of the materials. Cu−Fe deformation in-situ composites, It is expected that Cu−Fe composites should be developed in the direction of multi-element alloying and combined thermo-mechanical treatment to obtain better comprehensive properties based on optimized preparation methods.

As a novel type of functional material, Cu−C composites have been widely used in many lubricating, conductive and catalytic application systems. The Cu−graphite composites material can be used as the engine brush material to achieve the best electrical conductivity and wear resistance to prolong their service life, while Cu−graphene composites have been widely used in super-capacitors, ion batteries, and biosensors. In particular, significant progress has been made in electromagnetic shielding and catalysis. With the development of new technologies, the properties and applications of copper−carbon composites will be further expanded. A breakthrough could be made in improving the comprehensive properties of Cu−C composites through the organic combination of microstructure design, multi-stage and multi-size hybrid reinforcement and numerical simulation. Therefore, it is essential to develop a new type of C material-reinforced CMCs to realize the integration of material structure and function.

CMCs have become a new class of novel materials; however, they are still imperfectly characterized, and research on these new materials accelerates rapidly. It is anticipated that the new knowledge on CMCs will expand quickly in the next decades. Although a lot of research on the potential applications of CMCs has been carried out, the applications are still confined in a limited number of engineering fields due to technological and economic issues. Theoretical and practical studies on the fabrication and properties of CMCs are still in progress. The ongoing advancement in processing technologies, such as 3D printing and digital manufacturing, offers significant potential for the development of CMCs. Additive manufacturing and digital manufacturing techniques are expected to enable precise control over the microstructure and quality of CMCs,

allowing for the design of composites with optimized properties. Future research should explore how these emerging technologies can be utilized to enhance the mechanical and electrical properties of CMCs while reducing production costs. In addition to traditional reinforcement methods, new approaches such as high hetero-deformation induced (HDI) strengthening and hardening could be explored. These novel mechanisms could provide a pathway to achieve the desired balance of high strength and conductivity. Investigating the potential of these mechanisms in CMCs could lead to the development of composites with superior performance characteristics. It could be expected that with the increasingly booming demand for high-performance materials and increasingly severe resource and environmental problems, the high performance and sustainability of CMCs will bring more significant opportunities for the development of composites and related industries.

CRediT authorship contribution statement

Zhu XIAO: Conceptualization, Validation, Formal analysis, Investigation, Writing − Original draft, Writing − Review & editing; **Yan-jun DING:** Conceptualization, Resources, Writing − Review & editing; **Ze-jun WANG:** Analysis, Review & editing; **Yan-lin JIA:** Conceptualization, Review & editing; **Yan-bin JIANG:** Validation, Formal analysis, Investigation; **Shen GONG:** Formal analysis; **Zhou LI:** Conceptualization, Review & editing.

Declaration of competing interest

The authors declare that they have no known competing financial interests or personal relationships that could have appeared to influence the work reported in this paper.

Acknowledgments

The authors acknowledge the financial support by the Key-Area Research and Development Program of Guangdong Province, China (No. 2024B0101080003), Hunan Provincial Natural Science Foundation of China (No. 2024JJ2076), and grants from the State Key Laboratory of Powder Metallurgy, Central South University, China.

References

[1] PAK J H, KIM G N, HWANG S G, KIM B S, NOH J P, HUH S C. Mechanical properties of Cu matrix composite fabricated by extrusion process [J]. Transactions of Nonferrous Metals Society of China, 2016, 26(10): 2679−2686.

[2] SHAO Zhen-yi, PAN Heng-kang, SHU Rui, JIANG Xiao-song, ZHU Min-hao. Microstructures and interfacial interactions of Al_2O_3 whiskers and graphene nano-platelets co-reinforced copper matrix composites [J]. Transactions of Nonferrous Metals Society of China, 2022, 32(9): 2935−2947.

[3] LI Zhou, XIAO Zhu, JIANG Yan-bin, LEI Qian, XIE Jian-xin. Composition design, phase transition and fabrication of copper alloys with high strength and electrical conductivity [J]. The Chinese Journal of Nonferrous Metals, 2019, 29(9): 2009−2049. (in Chinese)

[4] AKBARPOUR M R, GAZANI F, MIRABAD H M, KHEZRI I, MOEINI A, SOHRABI N, KIM H S. Recent advances in processing, and mechanical, thermal and electrical properties of Cu−SiC metal matrix composites prepared by powder metallurgy [J]. Progress in Materials Science, 2023, 140: 101191.

[5] FALAH E N, PRATIWI V M, ADITYAWAN I, SAFRIDA N, WIKANDARI E, WIDIYANTO A R, ABDULLAH R. Research progress, potentials, and challenges of copper composite for metal injection moulding feedstock [J]. Powder Technology, 2024, 440: 119785.

[6] HUANG Wen-bing, YU Hao-jie, WANG L, WU Xu-dong, OUYANG Chen-guang, ZHANG Yan-hui, HE Jia-wen. State of the art and prospects in sliver-and copper-matrix composite electrical contact materials [J]. Materials Today Communications, 2023, 37: 107256.

[7] CANAKCI A, ARSLAN F, VAROL T. Physical and mechanical properties of stir-casting processed AA2024/B_4C_p composites [J]. Science and Engineering of Composite Materials, 2014, 21(4): 505−515.

[8] SANESH K, SUNDER S S, RADHIKA N. Effect of reinforcement content on the adhesive wear behavior of Cu10Sn5Ni/Si3N4 composites produced by stir casting [J]. International Journal of Minerals, Metallurgy, and Materials, 2017, 24(17): 1052−1060.

[9] DALMIS R, CUVALCI H, CANAKCI A, GULER O. Effect of nano-sized B_4C addition on the mechanical properties of ZA27 composites [J]. Journal of Wuhan University of Technology (Mater Sci Ed), 2017, 32(4): 747−752.

[10] GÜLER O, ÇUVALCı H, GÖKDAĞ M, ÇANAKÇI A, ÇELEBI M. Tribological behavior of ZA27/Al_2O_3/graphite hybrid nanocomposites [J]. Particulate Science and Technology, 2018, 36(7): 899−907.

[11] GÜLER O, CUVALCI H, CANAKCI A, CELEBI M. The effect of nano graphite particle content on the wear behaviour of ZA27 based hybrid composites [J]. Advanced Composites Letters, 2017, 26(2): 30−36.

[12] CANAKCI A, VAROL T. Microstructure and properties of AA7075/Al−SiC composites fabricated using powder metallurgy and hot pressing [J]. Powder Technology, 2014, 268: 72−79.

[13] ASADI P, FARAJI G, BESHARATI M K. Producing of AZ91/SiC composite by friction stir processing (FSP) [J]. The International Journal of Advanced Manufacturing

Technology, 2010, 51: 247−260.

[14] SEIFOLLAHZADEH P, ALIZADEH M, ABBASI M R. Strength prediction of multi-layered copper-based composites fabricated by accumulative roll bonding [J]. Transactions of Nonferrous Metals Society of China, 2021, 31(6): 1729−1739.

[15] WANG Lin, DU Qing-lin, LI Chang, CUI Xiao-hui, ZHAO Xing, YU Hai-liang. Enhanced mechanical properties of lamellar Cu/Al composites processed via high-temperature accumulative roll bonding [J]. Transactions of Nonferrous Metals Society of China, 2019, 29(8): 1621−1630.

[16] MELCHER R, TRAVITZKY N, ZOLLFRANK C, GREIL P. 3D printing of Al_2O_3/Cu−O interpenetrating phase composite [J]. Journal of Materials Science, 2011, 46(1): 1203−1210.

[17] XU De-xing, YANG Chang-lin, ZHAO Kang-ning, LI Hong-xiang, ZHANG Ji-shan. Interfacial microstructure and mechanical behavior of Mg/Cu bimetal composites fabricated by compound casting process [J]. Transactions of Nonferrous Metals Society of China, 2019, 29(6): 1233−1241.

[18] GHASALI E, EBADZADEH T, ALIZADEH M, RAZAVI M. Mechanical and microstructural properties of WC-based cermets: A comparative study on the effect of Ni and Mo binder phases [J]. Ceramics International, 2018, 44(2): 2283−2291.

[19] ZHAO Yu-chao, TANG Jian-cheng, YE Nan, ZHOU Wei-wei, WEI Chao-long, LIU Ding-jun. Influence of additives and concentration of WC nanoparticles on properties of WC−Cu composite prepared by electroplating [J]. Transactions of Nonferrous Metals Society of China, 2020, 30(6): 1594−1604.

[20] ZHOU Jin, MA Chao, KANG Xiao, ZHANG Lei, LIU Xin-li. Effect of WS_2 particle size on mechanical properties and tribological behaviors of Cu−WS_2 composites sintered by SPS [J]. Transactions of Nonferrous Metals Society of China, 2018, 28(6): 1176−1185.

[21] MOUSTAFA E B, TAHA M A. Evaluation of the microstructure, thermal and mechanical properties of Cu/SiC nanocomposites fabricated by mechanical alloying [J]. International Journal of Minerals, Metallurgy and Materials, 2021, 28(3): 475−486.

[22] SUN Jing, WANG Xu-qin, CHEN Yan, WANG Fei, WANG Hao-wei. Effect of Cu element on morphology of TiB_2 particles in TiB_2/Al−Cu composites [J]. Transactions of Nonferrous Metals Society of China, 2020, 30(5): 1148−1156.

[23] DING Hai-min, MIAO Wen-zhi, HUANG Xiao-wei, LIU Qing, FAN Xiao-liang, WANG Hui-qiang, CHU Kai-yu, LI Chun-yan. Influence of Al addition on microstructures of Cu−B alloys and Cu−ZrB_2 composites [J]. Transactions of Nonferrous Metals Society of China, 2020, 30(5): 1335−1346.

[24] ZHOU Tao, CHEN Wei, JIANG Yan-bin, QIU Wen-ting, CHEN Cai, XIAO Xu, QIN Liu-xin, GONG Shen, JIA Yan-lin, LI Zhou. Microstructure, properties and reaction kinetics of a Cu−Al_2O_3−TiB_2 alloy prepared by a new liquid phase in-situ reaction technology [J]. Journal of Materials Research and Technology, 2023, 26: 4024−4041.

[25] XIANG Ting, DAI Jie, QIU Wen-ting, WANG Ming-pu, LI Zhou, XIAO Zhu, JIANG Yan-bin. Cu/SiC_P composites prepared by in-situ carbonization synthesis [J]. JOM, 2019, 71: 2513−2521.

[26] ZHANG Xiao-xin, YUAN Ying-li, ZHAO San-qing, ZHANG Jun, YAN Qing-zhi. Microstructure stability, softening temperature and strengthening mechanism of pure copper, CuCrZr and Cu−Al_2O_3 up to 1000 °C [J]. Nuclear Materials and Energy, 2022, 30: 101123.

[27] ĎURIŠINOVÁ K, ĎURIŠIN J, ĎURIŠIN M. Microstructure and properties of nanocrystalline copper strengthened by a low amount of Al_2O_3 nanoparticles [J]. Journal of Materials Engineering and Performance, 2017, 26: 1057−1061.

[28] LI Cheng-guang, XIE Yue-hang, ZHOU Deng-shan, ZENG Wei, WANG Jun, LIANG Jia-miao, ZHANG De-liang. A novel way for fabricating ultrafine grained Cu−4.5vol.%Al_2O_3 composite with high strength and electrical conductivity [J]. Materials Characterization, 2019, 155: 109775.

[29] JIANG Chang, LIU Ze-kai, QIN Dan, LIU Tao, ZHANG Xue-hui, ZENG Long-fei, ZHAO Wen-min, LIU Bai-xiong, ZHANG Li-na. Preparation and microstructure of Cu−Al_2O_3 composites by a novel supercritical water liquid phase in-situ reaction method [J]. Materials Today Communications, 2024, 39: 108983.

[30] SONG Hong-yi, MAI Jun-jie, ZHANG Ze-quan, GU An-ping, MAI Yong-jin, CHANG Yong-qin. A high strength and high electrical conductivity copper based composite enhanced by graphene and Al_2O_3 nanoparticles [J]. Materials Science and Engineering A, 2024, 899: 146432.

[31] ZHANG Xue-hui, LI Xiao-xian, CHEN Hao, LI Tian-bai, SU Wei, GUO Sheng-da. Investigation on microstructure and properties of Cu−Al_2O_3 composites fabricated by a novel in-situ reactive synthesis [J]. Materials & Design, 2016, 92: 58−63.

[32] SHEHATA F, FATHY A, ABDELHAMEED M, MOUSTAFA S. Preparation and properties of Al_2O_3 nanoparticle reinforced copper matrix composites by in situ processing [J]. Materials & Design, 2009, 30(7): 2756−2762.

[33] ZHOU Deng-shan, ZENG Wei, ZHANG De-liang. A feasible ultrafine grained Cu matrix composite microstructure for achieving high strength and high electrical conductivity [J]. Journal of Alloys and Compounds, 2016, 682: 590−593.

[34] GÜLER O, VAROL T, ALVER Ü, CANAKCI A. Effect of Al_2O_3 content and milling time on the properties of silver coated Cu matrix composites fabricated by electroless plating and hot pressing [J]. Materials Today Communications, 2020, 24: 101153.

[35] SADOUN A M, MESELHY A F, ABDALLAH A W. Micro-structural, mechanical and wear behavior of electroless assisted silver coated Al_2O_3−Cu nanocomposites [J]. Materials Chemistry and Physics, 2021, 266: 124562.

[36] ZHAO Zi-qian, XIAO Zhu, LI Zhou, ZHU Meng-nan, YANG Zi-qi. Characterization of dispersion strengthened copper alloy prepared by internal oxidation combined with mechanical alloying [J]. Journal of Materials Engineering and Performance, 2017, 26(11): 1−7.

[37] XIANG Zi-qi, LEI Qian, XIAO Zhu, PANG Yong. Investigation on the microstructure and mechanical properties of Cu−2.7%Al_2O_3 dispersion strengthened copper

alloy [J]. Mining Metallurgical Engineering, 2014, 25(2): 444−450. (in Chinese)

[38] PAN Shuai-hang, ZHENG Tian-qi, YAO Gong-cheng, CHI Yi-tian, de ROSA I, LI Xiao-chun. High-strength and high-conductivity in situ Cu−TiB_2 nanocomposites [J]. Materials Science and Engineering A, 2022, 831: 141952.

[39] SHI Hao, ZHAO Yang, GAO Huai-bao, ZHANG Ming-shu, JIANG Yi-hui, CAO Fei, ZOU Jun-tao, LIANG Shu-hua. In-situ spherical TiB_2/Cu composite powder: A new method of liquid phase reaction coupled with gas atomization [J]. Materials Characterization, 2022, 191: 112096.

[40] MURMU U K, GHOSH A, SEIKH A H, ALNASER I A, ABDO H S, ALOWAYSI N S, GHOSH M. Mechanical alloying of ball-milled Cu−Ti−B elemental powder with the in situ formation of titanium diboride [J]. Metals, 2022, 12(12): 2108.

[41] ZOU Cun-lei, CHEN Zong-ning, KANG Hui-jun, WANG Wei, LI Ren-geng, LI Ting-ju, WANG Tong-min. Study of enhanced dry sliding wear behavior and mechanical properties of Cu−TiB_2 composites fabricated by in situ casting process [J]. Wear, 2017, 392: 118−125.

[42] CHEN Dan, JIANG Yi-hui, LI Yu-fa, LIU Di, HE Jiang-tan, CAO Fei, LIANG Shu-hua. In situ TiB_2/Cu composites fabricated by spray deposition using solid-liquid and liquid−liquid reactions [J]. Transactions of Nonferrous Metals Society of China, 2020, 30(7): 1849−1856.

[43] JIANG Yi-hui, WANG Ding-wen, XU Ying-qin, CAO Fei, LIANG Shu-hua. Fabrication and properties of in situ heterogeneous Cu/TiB_2 composites with a harmonic structure [J]. Materials Letters, 2020, 263: 127032.

[44] FENG Jiang, SONG Ke-xing, LIANG Shu-hua, GUO Xiu-hua, JIANG Yi-hui. Electrical wear of TiB_2 particle-reinforced Cu and Cu−Cr composites prepared by vacuum arc melting [J]. Vacuum, 2020, 175: 109295.

[45] BAHADOR A, UMEDA J, YAMANOGLU R, GHANDVAR H, ISSARIYAPAT A, ABU BAKAR T A, KONDOH K. Deformation mechanism and enhanced properties of Cu−TiB_2 composites evaluated by the in-situ tensile test and microstructure characterization [J]. Journal of Alloys and Compounds, 2020, 847: 156555.

[46] LI Zhou, XIAO Zhu, GUO Ming-xing, WANG Ming-pu, GONG Zhu-qing. Study on Cu−TiB_2 in situ composite prepared by liquid-metal mixing and rapid solidification process [J]. Transactions of Materials Heat Treatment, 2006, 27(5): 6−9. (in Chinese)

[47] GUO Ming-xing, SHEN Kun, WANG Ming-pu. Relationship between microstructure, properties and reaction conditions for Cu−TiB_2 alloys prepared by in situ reaction [J]. Acta Materialia, 2009, 57(15): 4568−4579.

[48] DINAHARAN I, SARAVANAKUMAR S, KALAISELVAN K, GOPALAKRISHNAN S. Microstructure and sliding wear characterization of Cu/TiB_2 copper matrix composites fabricated via friction stir processing [J]. Journal of Asian Ceramic Societies, 2017, 5(3): 295−303.

[49] AKBARPOUR M R, ASL F G, MIRABAD H M, KIM H. Microstructural characterization and enhanced tensile and tribological properties of Cu−SiC nanocomposites developed by high-pressure torsion [J]. Journal of Materials Research and Technology, 2022, 20: 4038−4051.

[50] AKBARPOUR M R, MIRABAD H M, GAZANI F, KHEZRI I, CHADEGANI A A, MOEINI A, KIM H S. An overview of friction stir processing of Cu−SiC composites: Microstructural, mechanical, tribological, and electrical properties [J]. Journal of Materials Research and Technology, 2023, 27: 1317−1349.

[51] CAO Xiao-ming, DUAN Jin, WANG Chao, JIN Peng, YANG Yong-jin, ZHANG Jin-song. Structure design and tribological properties of Cu−SiC foam ceramic composites [J]. Ceramics International, 2024, 50(5): 7366−7373.

[52] AKBARPOUR M R, SALAHI E, HESARI F A, YOON E Y, KIM H S, SIMCHI A. Microstructural development and mechanical properties of nanostructured copper reinforced with SiC nanoparticles [J]. Materials Science and Engineering A, 2013, 568: 33−39.

[53] ABD EL AAL M I. Effect of high-pressure torsion processing on the microstructure evolution and mechanical properties of consolidated micro size Cu and Cu−SiC powders [J]. Advanced Powder Technology, 2017, 28(9): 2135−2150.

[54] BAZARNIK P, NOSEWICZ S, ROMELCZYK-BAISHYA B, CHMIELEWSKI M, NĘDZA A S, MAJ J, HUANG Y, LEWANDOWSKA M, LANGDON T G. Effect of spark plasma sintering and high-pressure torsion on the microstructural and mechanical properties of a Cu−SiC composite [J]. Materials Science and Engineering A, 2019, 766: 138350.

[55] MA Guo-zheng, HE Peng-fei, WANG Hai-dou, TIAN Hong-gang, ZHOU Li, YONG Qing-song, LIU Ming, ZHAO Hai-chao, HE Dong-yu. Promoting bonding strength between internal Al−Si based gradient coating and aluminum alloy cylinder bore by forming homo-epitaxial growth interface [J]. Materials & Design, 2023, 227: 111764.

[56] KARTHIK B M, GOWRISHANKAR M C, SHARMA S, HIREMATH P, SHETTAR M, SHETTY N. Coated and uncoated reinforcements metal matrix composites characteristics and applications — A critical review [J]. Cogent Engineering, 2020, 7(1): 1856758.

[57] WĘGLEWSKI W, PITCHAI P, CHMIELEWSKI M, GURUPRASAD P, BASISTA M. Thermal conductivity of Cu-matrix composites reinforced with coated SiC particles: Numerical modeling and experimental verification [J]. International Journal of Heat and Mass Transfer, 2022, 188: 122633.

[58] CHEN Guang-jun, GUO Sheng-da, ZHANG Hai-hui, XIONG Hui-hui, GAN Lei. The effects of active elements on adhesion strength of SiC/Cu interface in SiC reinforced Cu-based composite: A first-principles investigation [J]. Materials Today Communications, 2022, 31: 103233.

[59] HU Ming, ZHANG Yun-long, TANG Li-li, SHAN Lin, GAO Jing, DING Pei-ling. Surface modifying of SiC particles and performance analysis of SiC_p/Cu composites [J]. Applied Surface Science, 2015, 332: 720−725.

[60] TODA-CARABALLO I, PEDRO R D D C. Modelling solid solution hardening in high entropy alloys [J]. Acta Materialia, 2015, 85: 14−23.

[61] LAURENT-BROCQ M, AKHATOVA A, PERRIÈRE L, CHEBINI S, SAUVAGE X, LEROY E, CHAMPION Y. Insights into the phase diagram of the CrMnFeCoNi high

entropy alloy [J]. Acta Materialia, 2015, 88: 355−365.

[62] ABHAYA S, RAJARAMAN R, KALAVATHI S, DAVID C, PANIGRAHI B K, AMARENDRA G. Effect of dose and post irradiation annealing in Ni implanted high entropy alloy FeCrCoNi using slow positron beam [J]. Journal of Alloys and Compounds, 2016, 669: 117−122.

[63] ÖKSÜZ K, ŞAHIN Y. Microstructure and hardness characteristics of Al_2O_3−B_4C particle-reinforced Cu matrix composites [J]. Acta Physica Polonica A, 2016, 129: 650−652.

[64] PANDEY V, SEETHARAM R, CHELLADURAI H. A comprehensive review: Discussed the effect of high-entropy alloys as reinforcement on metal matrix composite properties, fabrication techniques, and applications [J]. Journal of Alloys and Compounds, 2024, 1002: 175095.

[65] CHEN Jian, NIU Peng-yun, WEI Ting, HAO Liang, LIU Yun-zi, WANG Xian-hui, PENG Yu-li. Fabrication and mechanical properties of AlCoNiCrFe high-entropy alloy particle reinforced Cu matrix composites [J]. Journal of Alloys and Compounds, 2015, 649: 630−634.

[66] YU Hao-yang, FANG Wei, CHANG Ruo-bin, JI Pu-guang, WANG Qing-zhou. Modifying element diffusion pathway by transition layer structure in high-entropy alloy particle reinforced Cu matrix composites [J]. Transactions of Nonferrous Metals Society of China, 2019, 29(11): 2331−2339.

[67] WĘGLOWSKI M S. Friction stir processing-state of the art [J]. Archives of civil and Mechanical Engineering, 2018, 18(1): 114−129.

[68] DIXIT S, MAHATA A, MAHAPATRA D R, KAILAS S V, CHATTOPADHYAY K. Multi-layer graphene reinforced aluminum−Manufacturing of high strength composite by friction stir alloying [J]. Composites Part B: Engineering, 2018, 136: 63−71.

[69] ZHU Rui, SUN Yu-meng, FENG Jia-cheng, GONG Wen-biao, LI Yu-peng. Effect of microstructure on mechanical properties of FeCoNiCrAl high entropy alloys particle reinforced Cu matrix surface composite prepared by FSP [J]. Journal of Materials Research and Technology, 2023, 27: 2695−2708.

[70] ZHU Rui, LI Yu-peng, SUN Yu-meng, FENG Jia-cheng, GONG Wen-biao, COMPOUNDS. Microstructure and properties of FeCoNiCrAl high-entropy alloy particle-reinforced Cu-matrix composites prepared via FSP [J]. Journal of Alloys and Compounds, 2023, 940: 168906.

[71] WU Jia-wei, TANG Xun-hui, ZHANG Xin-ming, CEN Xi, GUO Bai-song, CHEN Biao, LI Wei, ZHANG Zhi-guo. Realizing the combination of high strength and good ductility of Cu matrix composites with CrCoNi reinforcement particles and microlaminated structure [J]. Journal of Alloys and Compounds, 2021, 872: 159632.

[72] YUAN Yuan, LI Zhou, XIAO Zhu, ZHAO Zi-qian, YANG Zi-qi. Microstructure evolution and properties of Cu−Cr alloy during continuous extrusion process [J]. Journal of Alloys and Compounds, 2017, 703: 454−460.

[73] JEONG Y B, JO H R, KIM J T, HONG S H, KIM K B. A study on the micro-evolution of mechanical property and microstructures in (Cu−30Fe)−2X alloys with the addition of minor alloying elements [J]. Journal of Alloys and Compounds, 2019, 786: 341−345.

[74] DING Yan-jun, DENG Zi-xuan, XIAO Zhu, FANG Mei, GONG Shen, QIU Wen-ting, WANG Xu. Effect of Nb content on mechanical reinforcement of the Cu−10Fe composites [J]. Journal of Alloys and Compounds, 2023, 966: 171540.

[75] ZHANG Ping, YUAN Xiao-bo, LI Yi-di, ZHOU Yun-he, LAI Rui-lin, LI Yun-ping, LEI Qian, CHIBA A. Influence of minor Ag addition on the microstructure and properties of powder metallurgy Cu−10wt.%Fe alloy [J]. Journal of Alloys and Compounds, 2022, 904: 163983.

[76] ZAARA K, CHEMINGUI M, OPTASANU V, KHITOUNI M. Solid solution evolution during mechanical alloying in Cu−Nb−Al compounds [J]. International Journal of Minerals, Metallurgy, and Materials, 2019, 26: 1129−1139.

[77] WANG Peng-fei, LIANG Ming, XU Xiao-yan, FENG Jian-qian, LI Cheng-shan, ZHANG Ping-xiang, LI Jin-shan. Effect of groove rolling on the microstructure and properties of Cu−Nb microcomposite wires [J]. International Journal of Minerals, Metallurgy, and Materials, 2021, 28: 279−284.

[78] CHUNG J H, SONG J S, HONG S I. Bundling and drawing processing of Cu−Nb microcomposites with various Nb contents [J]. Journal of Materials Processing and Technology, 2001, 113(1/2/3): 604−609.

[79] SPITZIG W A, DOWNING H L, LAABS F C, GIBSON E D, VERHOEVEN J D. Strength and electrical conductivity of a deformation-processed Cu−5%Nb composite [J]. Metallurgical Transactions A, 1993, 24: 7−14.

[80] PELTON A R, LAABS F C, SPITZIG W A, CHENG C C. Microstructural analysis of in-situ Cu−Nb composite wires [J]. Ultramicroscopy, 1987, 22(1/2/3/4): 251−265.

[81] HERINGHAUS F, RAABE D. Recent advances in the manufacturing of copper-base composites [J]. Journal of Materials Processing and Technology, 1996, 59(4): 367−372.

[82] BEVK J, HARBISON J P, BELL J L. Anomalous increase in strength of in situ formed Cu−Nb multifilamentary composites [J]. Journal of Applied Physics, 1978, 49(12): 6031−6038.

[83] HONG S I, KIM H S, HILL M A. Strength and ductility of heavily drawn bundled Cu−Nb filamentary microcomposite wires with various Nb contents [J]. Metallurgical and Materials Transactions A, 2000, 31: 2457−2462.

[84] VERHOEVEN J D, SPITZIG W A, SCHMIDT F A, KROTZ P D, GIBSON E D. Processing to optimize the strength of heavily drawn Cu−Nb alloys [J]. Journal of Materials Science, 1989, 24(3): 1015−1020.

[85] LEI Ruo-shan, WANG Ming-pu, LI Zhou, WEI Hai-gen, YANG Wen-chao, JIA Yan-lin, GONG Shen. Structure evolution and solid solubility extension of copper-niobium powders during mechanical alloying [J]. Materials Science and Engineering A, 2011, 528(13/14): 4475−4481.

[86] LIANG Ming, WANG Peng-fei, XU Xiao-yan, JIAO Gao-feng, LI Cheng-shan, ZHANG Ping-xiang. Thermal stability of high strength and high conductivity Cu−Nb microcomposites [J]. Rare Metal Materials and Engineering, 2017, 46(2): 382−386.

[87] DONG Zhi-lei, PENG Yi-fei, TAN Zhan-qiu, FAN Gen-lian, GUO Qiang, LI Zhi-qiang, XIONG Ding-bang. Simultaneously enhanced electrical conductivity and strength

in Cu/graphene/Cu sandwiched nanofilm [J]. Scripta Materialia, 2020, 187(1): 296−300.

[88] DING Chao-gang, XU Jie, SHAN De-bin, GUO Bin, LANGDON T G. Sustainable fabrication of Cu/Nb composites with continuous laminated structure to achieve ultrahigh strength and excellent electrical conductivity [J]. Composites Part B: Engineering, 2021, 211(7): 108662.

[89] KIM S I, LEE K H, MUN H A, KIM H S, HWANG S W, ROH J W, YANG D J, SHIN W H, LI X S, LEE Y H, SNYDER G J, KIM S W. Dense dislocation arrays embedded in grain boundaries for high-performance bulk thermoelectrics [J]. Science, 2015, 348(6230): 109−114.

[90] YAO Zai-qi, GE Ji-ping, LIU Shu-hua. Strength and conductivity of deformation-processed Cu−11.5Fe in suit composite [J]. Journal of Composite Materials, 2005, 22(3): 121−126.

[91] LIU K M, LU D P, ZHOU H T, CHEN Z B, ATRENS A, LU L. Influence of a high magnetic field on the microstructure and properties of a Cu−Fe−Ag in situ composite [J]. Materials and Science Engineering A, 2013, 584: 114−120.

[92] WANG Feng-ling, WAKOH K, LI Yun-ping, ITO S, YAMANAKA K, KOIZUMI Y, CHIBA A. Study of microstructure evolution and properties of Cu−Fe microcomposites produced by a pre-alloyed powder method [J]. Materials & Design, 2017, 126: 64−72.

[93] CHOI W M, HONG S I. High pressure torsioning of Cu−9Fe−1.2X (X=Co, Ni, Ag) microcomposites and their microstructural and mechanical evolution [J]. Advanced Materials Research, 2013, 813: 87−90.

[94] VERHOEVEN J D, CHUEH S C, GIBSON E D. Strength and conductivity of in situ Cu−Fe alloys [J]. Journal of Materials Science, 1989, 24: 1748−1752.

[95] GAO Hai-yan, WANG Jun, SHU Da, SUN Bao-de. Microstructure and properties of Cu−11Fe−6Ag in situ composite after thermo-mechanical treatments [J]. Journal of Alloys and Compounds, 2007, 438(1/2): 268−273.

[96] ZHANG Ping, LEI Qian, YUAN Xiao-bo, SHENG Xiao-fei, JIANG Dong, LI Yun-ping, LI Zhou. Microstructure and mechanical properties of a Cu−Fe−Nb alloy with a high product of the strength times the elongation [J]. Materials Today Communications, 2020, 25: 101353.

[97] JO H R, KIM J T, HONG S H, KIM Y S, PARK H J, PARK W J, PARK J M, KIM K B. Effect of silicon on microstructure and mechanical properties of Cu−Fe alloys [J]. Journal of Alloys and Compounds, 2017, 707: 184−188.

[98] MA Tao, LI Yun-gang. Research progress on Cu−Fe alloys [J]. Foundry Technology, 2016, 7(1): 1311−1314.

[99] WANG Meng, YANG Qian-ru, JIANG Yan-bing, LI Zhou, XIAO Zhu, GONG Shen, WANG Yong-ru, GUO Chuang-li, WEI Hai-gen. Effects of Fe content on microstructure and properties of Cu−Fe alloy [J]. Transactions of Nonferrous Metals Society of China, 2021, 31(10): 3039−3049.

[100] GUO Ming-xing, WANG Fei, YI Long. The microstructure controlling and deformation behaviors of Cu−Fe−C alloy prepared by rapid solidification [J]. Materials Science and Engineering A, 2016, 657: 197−209.

[101] WANG Meng, ZHANG Rui, XIAO Zhu, GONG Shen, JIANG Yan-bing, LI Zhou. Microstructure and properties of Cu−10wt.%Fe alloy produced by double melt mixed casting and multi-stage thermomechanical treatment [J]. Journal of Alloys and Compounds, 2020, 820: 153323.

[102] DING Yan-jun, WANG Xu, XIAO Zhu, FANG Mei, GONG Shen, QIU Wen-ting. Effect of cryogenic rolling and intermediate aging on mechanical reinforcement of the Cu−Fe−Nb composites [J]. Materials Characterization, 2024, 207: 113469.

[103] YUAN Da-wei, ZENG Hao, XIAO Xiang-peng, WANG Hang, HAN Bao-jun, LIU Bai-xiong, YANG Bin. Effect of Mg addition on Fe phase morphology, distribution and aging kinetics of Cu−6.5Fe alloy [J]. Materials Science and Engineering A, 2021, 812: 141064.

[104] LIU Ke-ming, HUANG Zhi-kai, ZHANG Xing-wang, LU De-ping, ATRENS A, ZHOU Hai-tao, YIN Yi, YU Jiu-ming, GUO Wei. Influence of Ag micro-alloying on the thermal stability and ageing characteristics of a Cu−14Fe in-situ composite [J]. Materials Science and Engineering A, 2016, 673: 1−7.

[105] SARKAR S, SRIVASTAVA C, CHATTOPADHYAY K. Development of a new class of high strength copper alloy using immiscibility route in Cu−Fe−Si system: Evolution of hierarchical multi-scale microstructure [J]. Materials Science and Engineering A, 2018, 723: 38−47.

[106] DING Yan-jun, XIAO Zhu, FANG Mei, GONG Shen, DAI Jie. Microstructure and mechanical properties of multi-scale α-Fe reinforced Cu−Fe composite produced by vacuum suction casting [J]. Materials Science and Engineering A, 2023, 864: 144603.

[107] ZHU Xue-feng, XIAO Zhu, AN J, JIANG Hong-yun, JIANG Yan-bin, LI Zhou. Microstructure and properties of Cu−Ag alloy prepared by continuously directional solidification [J]. Journal of Alloys and Compounds, 2021, 883: 160769.

[108] GUO Bao-jiang, ZHOU Yan-jun, ZHANG Yan-min, KONG Lin-bao, KANG Jun-wei, SONG Ke-xing, CAO Jun, ZHOU Zhi-yun. Effect of aging time on properties and nano precipitates characteristics of Cu−3.5Ag alloy [J]. Transactions of Materials and Heat Treatment, 2020, 41(6): 55−61.

[109] ZHANG Chao-min, SONG Ke-xing, CHENG Chu, ZHOU Yan-jun, MI Xu-jun, LI Zhou, XIAO Zhu, KONG Ling-bao, KANG Jun-wei, YUAN Peng-fei. Effect of large plastic deformation caused by cold-drawing on microstructure and properties of directional solidification Cu−4mass%Ag alloy [J]. Transactions of Materials and Heat Treatment, 2020, 41(12): 49−56.

[110] ZHAO Cong-cong, NIU Rong-mei, XIN Yan, BROWN D, MCGUIRE D, WANG En-gang, HAN Ke. Improvement of properties in Cu−Ag composites by doping induced microstructural refinement [J]. Materials Science and Engineering A, 2021, 799: 140091.

[111] LI Rui, ZUO Xiao-wei, WANG En-gang. Influence of thermomechanical process and Fe addition on microstructural evolution and properties of Cu−26wt.%Ag composite [J]. Journal of Alloys and Compounds, 2019, 773: 121−130.

[112] LIU Jia-bin, ZHANG Lei, MENG Liang. Effects of rare-earth additions on the microstructure and strength of Cu−Ag composites [J]. Materials Science and Engineering A, 2008, 498(1/2): 392−396.

[113] ZHANG Xiao-hui, NING Yuan-tao, LI Yong-nian, DAI Hong, YANG Jia-ming. Microstructure and properties of heavily deformed Cu−10Ag in-situ filamentary composite [J]. Chinese Journal of Nonferrous Metals, 2002, 12(1): 15−23. (in Chinese)

[114] ZHANG Lei, MENG Liang, LIU Jia-bin. Effects of Cr addition on the microstructural, mechanical and electrical characteristics of Cu−6wt.%Ag microcomposite [J]. Scripta Materialia, 2005, 52(7): 587−592.

[115] LI Rui, WANG En-gang, ZUO Xiao-wei. Co-precipitation, strength and electrical resistivity of Cu−26wt.%Ag−0.1wt.%Fe alloy [J]. Materials, 2017, 10(12): 1383.

[116] DENG Jian-qi, ZHANG Xiu-qing, SHANG Shu-zhen, LIU Fu, ZHAO Zu-xin, YE Yi-fu. Effect of Zr addition on the microstructure and properties of Cu−10Cr in situ composites [J]. Materials & Design, 2009, 30(10): 4444−4449.

[117] ZHOU Hai-bin, YAO Ping-ping, XIAO Ye-long, FAN Kun-yang, GONG Tai-ming, ZHAO Lin, ZHANG Zhong-yi, DENG Min-wen, LI Yu-xing. High energy braking behaviors and tribo-map constructions of Cu metal matrix composites with different Cr volume contents [J]. Wear, 2022, 496: 204275.

[118] ZHANG Xiang-feng, GUO Xiu-hua, SONG Ke-xing, WANG Xu, FENG Jiang, LI Shao-lin, LIN Huan-ran. Simulation and verification of thermal conductivity of CuCr30 contact material based on morphological changes of Cr particles [J]. Materials Today Communications, 2021, 26: 102153.

[119] TIAN Wei, BI Li-ming, MA Feng-cang, DU Jian-di. Effect of Zr on as-cast microstructure and properties of Cu−Cr alloy [J]. Vacuum, 2018, 149: 238−247.

[120] MENG Ao, NIE Jin-feng, WEI Kang, KANG Hui-jun, LIU Zhang-jia, ZHAO Yong-hao. Optimization of strength, ductility and electrical conductivity of a Cu−Cr−Zr alloy by cold rolling and aging treatment [J]. Vacuum, 2019, 167: 329−335.

[121] ZHOU Zhin-ming, WANG Ya-ping, GAO Jin-rong, KOLBE M. Microstructure of rapidly solidified Cu−25wt.%Cr alloys[J]. Materials Science and Engineering A, 2005, 398(1/2): 318−322.

[122] HAMEDAN S S, ABDI M, SHEIBANI S. Comparative study on hot rolling of Cu−Cr and Cu−Cr−CNT nanocomposites [J]. Transactions of Nonferrous Metals Society of China, 2018, 28(10): 2044−2052.

[123] LIU Ke-ming, LU De-ping, ZHOU Hhai-tao, ATRENS A, CHEN Zhin-bao, ZOU Jin, ZENG Sn-min. Influence of Ag micro-alloying on the microstructure and properties of Cu−7Cr in situ composite [J]. Journal of Alloys and Compounds, 2010, 500(2): L22−L25.

[124] MAO Qing-zhong, WANG Long, NIE Jin-feng, ZHAO Yong-hao. Enhancing strength and electrical conductivity of Cu-Cr composite wire by two-stage rotary swaging and aging treatments [J]. Composites Part B: Engineering, 2022, 231: 109567.

[125] ZOU Qing-chuan, WU Da, AN Xi-zhong, LI Meng, XU Chang-yuan, ZHOU Xiang-lin, JIE Jin-chuan, DONG Zong-hui. Fabrication of W−20Cu composite with optimization of particle packing in PM route [J]. Journal of Materials Research and Technology, 2022, 19: 2895−2906.

[126] ZHUO Long-chao, SUN Jia-cheng, ZHANG Qi-qi, ZHANG Yi-heng, LIANG Shu-hua, TANG Yu-ling. Hierarchical tungsten-copper composite reinforced by a concrete skeleton of particulate and fibrous tungsten with coherent Cr precipitates in the copper matrix [J]. Materials Characterization, 2022, 184: 111670.

[127] PERVIKOV A, FILIPPOV A, MIRONOV Y, KALASHNIKOV M, KRINITCYN M, ESKIN D, LERNER M, TARASOV S. Microstructure and properties of a nanostructured W−31wt.%Cu composite produced by magnetic pulse compaction of bimetallic nanoparticles [J]. International Journal of Refractory Metals and Hard Materials, 2022, 103: 105735.

[128] AI Yong-ping. Preparation of Cu−W film by ion beam sputtering and characterization [J]. Chemical Physics Letters, 2017, 690: 1−4.

[129] LIU Dong-guang, MA Hao-ran, RUAN Chong-fei, LUO Lai-ma, MA Yong, WANG Zu-min, WU Yu-cheng. Interface diffusion and mechanical properties of ODS-W/Cu prepared by spark plasma sintering [J]. Vacuum, 2021, 190: 110278.

[130] CHEN Yuan-yuan, HUANG Yuan, LI Fei, HAN Lu, LIU Dong-guang, LUO Lai-ma, MA Zong-qing, LIU Yong-chang, WANG Zu-min. High-strength diffusion bonding of oxide-dispersion-strengthened tungsten and CuCrZr alloy through surface nano-activation and Cu plating [J]. Journal of Materials Science and & Technology, 2021, 92: 186−194.

[131] ZHANG Lian-meng, CHEN Wen-shu, LUO Guo-qiang, CHEN Ping-an, SHEN Qiang, WANG Cuan-bin. Low-temperature densification and excellent thermal properties of W−Cu thermal-management composites prepared from copper-coated tungsten powders [J]. Journal of Alloys and Compounds, 2014, 588: 49−52.

[132] ZHANG Cong-lin, GAO Qi, LV Peng, CAI Jie, PENG Ching-tun, JIN Yun-xue, GUAN Qing-feng. Surface modification of Cu−W powder metallurgical alloy induced by high-current pulsed electron beam [J]. Powder Technology, 2018, 325: 340−346.

[133] LI Xiu-qing, WANG Qi, WEI Shi-zhong, LOU Wen-peng, XU Liu-jie, ZHOU Yu-cheng. Microstructure and characteristics of Cu−W composite prepared by W-coated Cu powder with different W contents [J]. Materials Science and Engineering A, 2024, 892: 146090.

[134] XIE Tian-le, ZHU Jia-jun, FU Li-cai, ZHANG Rui-ling, LI Na, YANG Meng-zhao, WANG Jia-le, QIN Wen, YANG Wu-lin, LI De-yi, ZHOU Ling-ping. The evolution of hardness in Cu−W alloy thin films [J]. Materials Science and Engineering A, 2018, 729: 170−177.

[135] SHIRVANIMOGHADDAM K, HAMIM S U, AKBARI M K, FAKHRHOSEINI S M, KHAYYAM H, PAKSERESHT A H, GHASALI E, ZABET M, MUNIR K S, JIA S A, DAVIM J P, NAEBE M. Carbon fiber reinforced metal matrix composites: Fabrication processes and properties [J]. Composites Part A: Applied Science and Manufacturing, 2017, 92: 70−96.

[136] WANG Cong-zhen, GAN Xue-ping, TAO Jing-mei, XIE Ming, YI Jian-hong, LIU Yi-chun. Simultaneous achievement of high strength and high ductility in copper matrix composites with carbon nanotubes/Cu composite foams as reinforcing skeletons [J]. Nanotechnology, 2020, 31(4): 045701.

[137] YANG Zi-yue, WANG Li-dong, SHI Zhen-dong, WANG Miao, CUI Ye, WEI Bing, XU Shi-chong, ZHU Yun-peng, FEI Wei-dong. Preparation mechanism of hierarchical layered structure of graphene/copper composite with ultrahigh tensile strength [J]. Carbon, 2018, 127: 329−339.

[138] ZANG Xiao-xian, SUN Chen-cheng, DAI Zi-yang, YANG Jun, DONG Xiao-chen. Nickel hydroxide nanosheets supported on reduced graphene oxide for high-performance supercapacitors [J]. Journal of Alloys and Compounds, 2017, 691: 144−150.

[139] LI Bing-qian, ZHANG Fu-qin, YANG Zhao, ZHENG Ji-xiang. Frictional wear properties of carbon-fiber-reinforced copper-based self-lubricating composites [J]. Mining and Metallurgical Engineering, 2016, 36(5): 107−114. (in Chinese)

[140] ALI S, AHMAD F, YUSOFF P S M M, MUHAMAD N, OÑATE E, RAZA M R, MALIK K. A review of graphene reinforced Cu matrix composites for thermal management of smart electronics [J]. Composites Part A: Applied Science and Manufacturing, 2021, 144: 106357.

[141] HUANG He-dong, PU Hao, FAN Jun-wei, SU Bing, LIU Hong-yung, HA Xin-yi, REN Yong-fei, GUO Ze-yu. Effect of metallic copper on the electrothermal properties of carbon nanofibers [J]. Carbon Letters, 2024, 34: 1259−1267.

[142] WANG Yi-ran, GAO Yi-min, TAKAHASHI J, WAN Yi, LI Meng-ting, XIAO Bing, ZHANG Yun-qian, HE Xiang-dong. Investigation of modification of Cu−Ni-graphite composite by silver [J]. Materials Chemistry and Physics, 2020, 239: 121990.

[143] BAI Lin, GE Yi-cheng, ZHU Lin-ying, CHEN Yi-han, YI Mao-zhong. Preparation and properties of copper-plated expanded graphite/copper composites [J]. Tribology International, 2021, 161: 107094.

[144] LI Heng-qing, LIU Yang-zhen, ZHENG Bao-chao, WANG Shuai, YI Yan-liang, ZHANG Yong-zhen, LI Wei. On the tribological behaviors of Cu matrix composites with different Cu-coated graphite content [J]. Journal of Materials Research and Technology, 2023, 25: 83−94.

[145] XIAO Zhu, CHEN Ru-shi, ZHU Xue-feng, LI Zhou, XU Guo-fu, JIA Yan-lin, ZHANG Yun-he. Microstructure, and physical and mechanical properties of copper−graphite composites obtained by in situ reaction method [J]. Journal of Materials Engineering and Performance, 2020, 29: 1696−1705.

[146] CHEN Ru-shi, XIAO Zhu, DAI Jie, LI Zhou, XU Guo-fu. Study on the relationship between the properties of copper graphite composite and the shape and particle size of graphite [J]. Nonferrous Metal Materials Engineering, 2019, 40(5): 1−7. (in Chinese)

[147] YANG Ming, WENG Lin, ZHU Han-xing, FAN Tong-xiang, ZHANG Di. Simultaneously enhancing the strength, ductility and conductivity of copper matrix composites with graphene nanoribbons [J]. Carbon, 2017, 118: 250−260.

[148] WANG Hong, SUN Xu, WANG Yi-zhou, LI Kun-cai, WANG Jing, DAI Xu, CHEN Bin, CHONG Dao-tong, ZHANG Liu-yang, YAN Jun-jie. Acid enhanced zipping effect to densify MWCNT packing for multifunctional MWCNT films with ultra-high electrical conductivity [J]. Nature Communications, 2023, 14(1): 380.

[149] ZHANG Shu-chen, QIAN Liu, ZHAO Qiu-chen, WANG Ze-qun, LIN De-wu, LIU Wei-ming, CHEN Ya-bin, ZHANG Jin. Carbon nanotube: Controlled synthesis determines its future [J]. Science China Materials, 2020, 63(1): 16−34.

[150] ALMANSOUR A, SACKSTEDER D, GORETSKI A J III, LIZCANO M. Novel processing, testing and characterization of copper/carbon nanotube (Cu/CNT) yarn composite conductor [J]. International Journal of Applied Ceramic Technology, 2023, 20(2): 917−937.

[151] ROBERT F, PRINCE A A, JAC FREDO A R. Investigation of using CNT and Cu/CNT wires for replacing Cu for power electronics and electrical applications [J]. ESC Journal of Solid State Science and Technology, 2022, 11(2): 023011.

[152] DHALL S, PUSHKARN S, KHARANGARH P. Synthesis and Structural studies of lightweight CNT/Cu composites: An overview [C]//IOP Conference Series: Materials Science and Engineering. Bristol, UK: IOP Puldishing Ltd, 2022: 012017.

[153] XU Le-le, JIAO Xin-yu, SHI Chao, WU An-ping, HOU Peng-xiang, LIU Chang, CHENG Hui-ming. Single-walled carbon nanotube/copper core-shell fibers with a high specific electrical conductivity [J]. ACS Nano, 2023, 17(10): 9245−9254.

[154] DANESHVAR F, CHEN H X, ZHANG T, SUE H J. Fabrication of light-weight and highly conductive copper−carbon nanotube core−shell fibers through interface design [J]. Advanced Materials Interfaces, 2020, 7(19): 2000779.

[155] DENG Hui, YI Jian-hong, XIA Chao, YI Yi. Mechanical properties and microstructure characterization of well-dispersed carbon nanotubes reinforced copper matrix composites [J]. Journal of Alloys and Compounds, 2017, 727: 260−268.

[156] WANG Dan, YAN An, LIU Yi-chun, WU Zhong, GAN Xue-ping, LI Feng-xian, TAO Jing-mei, LI Cai-ju, YI Jian-hong. Interfacial bonding improvement through nickel decoration on carbon nanotubes in carbon nanotubes/Cu composite foams reinforced copper matrix composites [J]. Nanomaterials, 2022, 12(15): 2548.

[157] JAYATHILAKA W A D M, CHINNAPPAN A, RAMAKRISHNA S. A review of properties influencing the conductivity of CNT/Cu composites and their applications in wearable/flexible electronics [J]. Journal of Materials Chemistry C, 2017, 5(36): 9209−9237.

[158] ZOU Jing-yun, LIU Dan-dan, ZHAO Jing-na, HOU Li-gan, LIU Tong, ZHANG Xiao-han, ZHAO Yong-hao, ZHU Yun-tian, LI Qing-wen. Ni nanobuffer layer provides light-weight CNT/Cu fibers with superior robustness, conductivity, and ampacity [J]. ACS Applied Materials and Interfaces, 2018, 10(9): 8197−8204.

[159] KIM C, LIM B, KIM B, SHIM U, OH S, SUNG B, CHOI J, KI J, BAIK S. Strengthening of copper matrix composites by nickel-coated single-walled carbon nanotube reinforcements [J]. Synthetic Metals, 2009, 159(5/6): 424−429.

[160] LI Hui-fang, YONG Zhen-zhong, LIU Dan-dan, WU Kun-jie, GUO Lei, WANG Xiao-na, JIN He-hua, LI Qing-wen. Interface engineering for high-strength and high-ampacity of carbon nanotube/copper composite wires [J]. Carbon, 2024, 219: 118845.

[161] WANG Rui, WAN Yi-zao, HE Fang, QI Yu, YOU Wei, LUO Hong-lin. The synthesis of a new kind of magnetic coating

on carbon fibers by electrodeposition [J]. Applied Surface Science, 2012, 258(7): 3007−3011.
[162] HAN Zhan-po, ZHANG Xiao-yan, YUAN Hua, LI Zhen-de, LI Guang-zhen, ZHANG Hua-yu, TAN Ye-qiang. Graphene oxide/gold nanoparticle/graphite fiber microelectrodes for directing electron transfer of glucose oxidase and glucose detection [J]. Journal of Power Sources, 2022, 521: 230956.
[163] VARENTSOVA V I, VARENSTOV V R, BATAEV I A, YUSIN S I. Effect of surface state of carbon fiber electrode on copper electroplating from sulfate solutions [J]. Protection of Metals and Physical Chemistry of Surfaces, 2011, 47: 43−47.
[164] ZHANG Guo-dong, YU Jun-wei, SU Chao, DI Cheng-rui, CI Sheng-zong, MOU Yuan-ming, FU Yun-guo, QIAO Kun. The effect of annealing on the properties of copper-coated carbon fiber [J]. Surfaces and Interfaces, 2023, 37: 102630.
[165] KIM K W, HAN W, KIM B S, KIM B J, AN K H. A study on EMI shielding enhancement behaviors of Ni-plated CFs-reinforced polymer matrix composites by post heat treatment [J]. Applied Surface Science, 2017, 415: 55−60.
[166] LYSENKO A A, MEDVEDEVA N G, GORBERG B L, KUZIKOVA I L, ASTASHKINA O V, UVAROVA N F. Silver-containing carbon fibers, preparation and properties [J]. Fibre Chemistry, 2021, 52(5): 324−329.
[167] SU Xing-hua, QIANG Cheng-wen. Electroless plating and magnetic properties of Co−Zn−P coating on short carbon fibres [J]. Bulletin of Materials Science, 2012, 35: 1093−1097.
[168] YU Ping, BOTTE G G. Bimetallic platinum-iron electrocatalyst supported on carbon fibers for coal electrolysis [J]. Journal of Power Sources, 2015, 274: 165−169.
[169] YI H, KIM J Y, GUL H Z, KANG S, KIM G, SIM E, JI H, KIM J, CHOI Y C, KIM W S, LIM S C. Wiedemann-Franz law of Cu-coated carbon fiber [J]. Carbon, 2020, 162: 339−345.
[170] DAOUSH W M, ALBOGMY T S, KHAMIS M A, INAM F. Syntheses and step-by-step morphological analysis of nano-copper-decorated carbon long fibers for aerospace structural applications [J]. Crystals, 2020, 10(12): 1090.
[171] TRAN T Q, LEE J K Y, CHINNAPPAN A, LOC N H, TRAN L T, JI D X, JAYATHILAKA W A D M, KUMAR V V, RAMAKRISHNA S. High-performance carbon fiber/gold/copper composite wires for lightweight electrical cables [J]. Journal of Materials Science and Technology, 2020, 42: 46−53.
[172] CAO Mu, XIONG Ding-bang, YANG Li, LI Shuai-shuai, XIE Yi-qun, GUO Qiang, LI Zhi-qiang, ADAMS H, GU Jia-jun, FAN Tong-xiang, ZHANG Di. Ultrahigh electrical conductivity of graphene embedded in metals [J]. Advanced Functional Materials, 2019, 29(17): 1806792.
[173] SHIN S E, CHOI H J, SHIN J H, BAE D H. Strengthening behavior of few-layered graphene/aluminum composites [J]. Carbon, 2015, 82: 143−151.
[174] GAO Zhao-shun, ZUO Ting-ting, WANG Mang, ZHANG Ling, DA Bo, RU Ya-dong, XUE Jiang-li, WU Yue, HAN Li, XIAO Li-ye. In-situ graphene enhanced copper wire: A novel electrical material with simultaneously high electrical conductivity and high strength [J]. Carbon, 2022, 186: 303−312.
[175] ZUO Ting-ting, XUE Jiang-li, RU Ya-dong, GAO Zhao-shun, ZHANG Ling, DA Bo, HAN Li, XIAO Li-ye. The improved softening resistance and high electrical conductivity of the 3D graphene enhanced copper-based composite fabricated by liquid carbon source [J]. Materials Letters, 2021, 283: 128895.
[176] WANG Miao, WANG Li-dong, SHENG Jie, YANG Zi-yue, SHI Zhen-dong, ZHU Yun-peng, LI Jie, FEI Wei-dong. Direct synthesis of high-quality graphene on Cu powders from adsorption of small aromatic hydrocarbons: A route to high strength and electrical conductivity for graphene/Cu composite [J]. Journal of Alloys and Compounds, 2019, 798: 403−413.

先进铜基复合材料的研究与发展

肖 柱[1,2]，丁燕军[1]，王泽军[1]，贾延林[1,2]，姜雁斌[1,2]，龚 深[1,2]，李 周[1,2]

1. 中南大学 材料科学与工程学院，长沙 410083；
2. 中南大学 有色金属材料科学与工程教育部重点实验室，长沙 410083

摘 要：铜基复合材料(CMCs)通过将纯铜与复合相的功能特性结合，展现出广阔的应用潜力。随着航空航天、微电子及智能终端技术的迅速发展，对具备优异力学和电性能 CMCs 的需求日益增长。本文综述了各种典型 CMCs 的设计原理、制备方法及组织与性能，总结了 Cu 基体中复合相的分布形态及其对显微组织演变和综合性能的影响，并深入探讨了其强化机制和机理。研究结果揭示了增强相与材料性能之间的内在关系，为开发综合性能更优的 CMCs 提供了重要的理论支持。最后，展望了 CMCs 的未来应用方向和发展趋势。

关键词：铜基复合材料；复合原理；增强相；强度；导电性

(Edited by Xiang-qun LI)